BRAIN
ORIGINAL ARTICLE

Gain-of-function and loss-of-function variants in *GRIA3* lead to distinct neurodevelopmental phenotypes

Berardo Rinaldi,[1,†] Allan Bayat,[2,3,4,†] Linda G. Zachariassen,[2,†] Jia-Hui Sun,[5,6,†] Yu-Han Ge,[5,7] Dan Zhao,[2] Kristine Bonde,[2] Laura H. Madsen,[2] Ilham Abdimunim Ali Awad,[2] Duygu Bagiran,[2] Amal Sbeih,[2] Syeda Maidah Shah,[2] Shaymaa El-Sayed,[2] Signe M. Lyngby,[2] Miriam G. Pedersen,[2] Charlotte Stenum-Berg,[2] Louise Claudia Walker,[8] Ilona Krey,[9] Andrée Delahaye-Duriez,[10,11,12] Lisa T. Emrick,[13,14] Krystal Sully,[13] Chaya N. Murali,[14] Lindsay C. Burrage,[14] Julie Ana Plaud Gonzalez,[13] Mered Parnes,[13,15] Jennifer Friedman,[16,17,18] Bertrand Isidor,[19] Jérémie Lefranc,[20] Sylvia Redon,[21,22] Delphine Heron,[23,24] Cyril Mignot,[23,24] Boris Keren,[25] Mélanie Fradin,[26] Christele Dubourg,[27,28] Sandra Mercier,[19,29] Thomas Besnard,[19,29] Benjamin Cogne,[19,29] Wallid Deb,[19,29] Clotilde Rivier,[30] Donatella Milani,[31] Maria Francesca Bedeschi,[1] Claudia Di Napoli,[1] Federico Grilli,[1] Paola Marchisio,[32,33] Suzanna Koudijs,[34] Danielle Veenma,[35] Emanuela Argilli,[36,37] Sally Ann Lynch,[38] Ping Yee Billie Au,[39] Fernando Eduardo Ayala Valenzuela,[40] Carolyn Brown,[41] Diane Masser-Frye,[42] Marilyn Jones,[42] Leslie Patron Romero,[43] Wenhui Laura Li,[44] Erin Thorpe,[41] Laura Hecher,[45] Jessika Johannsen,[45] Jonas Denecke,[45] Vanda McNiven,[46,47] Anna Szuto,[46,48] Emma Wakeling,[49] Vincent Cruz,[50] Valerie Sency,[50] Heng Wang,[50] Juliette Piard,[51,52] Fanny Kortüm,[53] Theresia Herget,[53] Tatjana Bierhals,[53] Angelo Condell,[54] Bruria Ben-Zeev,[55,56] Simranpreet Kaur,[54,57] John Christodoulou,[54,57,58,59] Amelie Piton,[60] Christiane Zweier,[61,62] Cornelia Kraus,[61] Alessia Micalizzi,[63] Marina Trivisano,[64] Nicola Specchio,[64] Gaetan Lesca,[65,66] Rikke S. Møller,[3,4] Zeynep Tümer,[67,68] Maria Musgaard,[8] Benedicte Gerard,[69] Johannes R. Lemke,[70] Yun Stone Shi[5,7,71] and Anders S. Kristensen[2]

[†]These authors contributed equally to this work.

AMPA (α-amino-3-hydroxy-5-methyl-4-isoxazole propionic acid) receptors (AMPARs) mediate fast excitatory neurotransmission in the brain. AMPARs form by homo- or heteromeric assembly of subunits encoded by the *GRIA1–GRIA4* genes, of which only *GRIA3* is X-chromosomal. Increasing numbers of *GRIA3* missense variants are reported in patients with neurodevelopmental disorders (NDD), but only a few have been examined functionally.

Here, we evaluated the impact on AMPAR function of one frameshift and 43 rare missense *GRIA3* variants identified in patients with NDD by electrophysiological assays. Thirty-one variants alter receptor function and show loss-of-function or gain-of-function properties, whereas 13 appeared neutral.

Received July 17, 2023. Revised October 17, 2023. Accepted November 09, 2023. Advance access publication December 1, 2023

We collected detailed clinical data from 25 patients (from 23 families) harbouring 17 of these variants. All patients had global developmental impairment, mostly moderate (9/25) or severe (12/25). Twelve patients had seizures, including focal motor (6/12), unknown onset motor (4/12), focal impaired awareness (1/12), (atypical) absence (2/12), myoclonic (5/12) and generalized tonic-clonic (1/12) or atonic (1/12) seizures. The epilepsy syndrome was classified as developmental and epileptic encephalopathy in eight patients, developmental encephalopathy without seizures in 13 patients, and intellectual disability with epilepsy in four patients. Limb muscular hypotonia was reported in 13/25, and hypertonia in 10/25. Movement disorders were reported in 14/25, with hyperekplexia or non-epileptic erratic myoclonus being the most prevalent feature (8/25).
Correlating receptor functional phenotype with clinical features revealed clinical features for *GRIA3*-associated NDDs and distinct NDD phenotypes for loss-of-function and gain-of-function variants. Gain-of-function variants were associated with more severe outcomes: patients were younger at the time of seizure onset (median age: 1 month), hypertonic and more often had movement disorders, including hyperekplexia. Patients with loss-of-function variants were older at the time of seizure onset (median age: 16 months), hypotonic and had sleeping disturbances. Loss-of-function and gain-of-function variants were disease-causing in both sexes but affected males often carried *de novo* or hemizygous loss-of-function variants inherited from healthy mothers, whereas affected females had mostly *de novo* heterozygous gain-of-function variants.

1 Medical Genetics Unit, Fondazione IRCCS Ca' Granda Ospedale Maggiore Policlinico, Milan 20122, Italy
2 Department of Drug Design and Pharmacology, University of Copenhagen, Copenhagen 2100, Denmark
3 Department of Epilepsy Genetics and Personalized Medicine, Danish Epilepsy Centre, Dianalund 4293, Denmark
4 Department of Regional Health Research, University of Southern Denmark, Odense 5230 Denmark
5 State Key Laboratory of Pharmaceutical Biotechnology, Model Animal Research Center, Department of Neurology, Nanjing Drum Tower Hospital, Medical School, Nanjing University, Nanjing 210032, China
6 Zhejiang Key Laboratory of Organ Development and Regeneration, College of Life and Environmental Sciences, Hangzhou Normal University, Hangzhou 310030, China
7 Ministry of Education Key Laboratory of Model Animal for Disease Study, National Resource Center for Mutant Mice, Jiangsu Key Laboratory of Molecular Medicine, Medical School, Nanjing University, Nanjing 210032, China
8 Department of Chemistry and Biomolecular Sciences, University of Ottawa, Ottawa K1H 8M5, Canada
9 Institute of Human Genetics, University of Leipzig Medical Center, Leipzig 04103, Germany
10 Unité fonctionnelle de médecine génomique et génétique clinique, Hôpital Jean Verdier, Assistance Publique des Hôpitaux de Paris, Bondy 93140, France
11 NeuroDiderot, UMR 1141, Inserm, Université Paris Cité, Paris 75019, France
12 UFR SMBH, Université Sorbonne Paris Nord, Bobigny 93000, France
13 Division of Neurology and Developmental Neurosciences, Department of Pediatrics, Baylor College of Medicine, Texas Children's Hospital, Houston, TX 77030, USA
14 Department of Molecular and Human Genetics, Baylor College of Medicine, Houston, TX 77030, USA
15 Pediatric Movement Disorders Clinic, Texas Children's Hospital and Baylor College of Medicine, Houston, TX 77030, USA
16 Rady Children's Institute for Genomic Medicine, San Diego, CA 92123, USA
17 Department of Neurosciences, University of California San Diego, San Diego, CA 92123, USA
18 Department of Pediatrics, University of California San Diego, San Diego, CA 92123, USA
19 Nantes Université, CHU Nantes, Service de Génétique Médicale, Nantes 44000, France
20 Pediatric Neurophysiology Department, CHU de Brest, Brest 29200, France
21 Service de Génétique Médicale, CHU de Brest, Brest 29200, France
22 Université de Brest, CHU de Brest, UMR 1078, Brest F29200, France
23 APHP Sorbonne Université, Département de Génétique, Hôpital Armand Trousseau and Groupe Hospitalier Pitié-Salpêtrière, Paris 75013, France
24 Centre de Référence Déficiences Intellectuelles de Causes Rares, Paris 75013, France
25 Genetic Department, APHP, Sorbonne Université, Pitié-Salpêtrière Hospital, Paris 75013, France
26 Service de Génétique Médicale, Hôpital Sud, CHU de Rennes, Rennes 35200, France
27 Service de Génétique Moléculaire et Génomique, CHU de Rennes, Rennes 35200, France
28 Université de Rennes, CNRS, Institut de Genetique et Developpement de Rennes, UMR 6290, Rennes 35200, France
29 Nantes Université, CHU Nantes, CNRS, INSERM, l'institut du thorax, Nantes 44000, France
30 Department of Paediatrics, Villefranche-sur-Saône Hospital, Villefranche-sur-Saône 69655, France
31 Fondazione IRCCS Ca' Granda Ospedale Maggiore Policlinico, Milan 20122, Italy
32 Fondazione IRCCS Ca' Granda Ospedale Maggiore Policlinico, Pediatria Pneumoinfettivologia, Milan 20122, Italy
33 University of Milan, Milan 20122, Italy

34 Department of Neurology, ENCORE, Erasmus Medical Center-Sophia Children's Hospital, Rotterdam 3015, The Netherlands
35 Department of Pediatrics, ENCORE, Erasmus Medical Center-Sophia Children's Hospital, Rotterdam 3015, The Netherlands
36 Institute of Human Genetics, University of California, San Francisco, CA 94143, USA
37 Department of Neurology, Weill Institute for Neurosciences, University of California, San Francisco, CA 94143, USA
38 Department of Clinical Genetics, Children's Health Ireland Crumlin, Dublin D12 N512, Ireland
39 Department of Medical Genetics, Alberta Children's Hospital Research Institute, Cumming School of Medicine, University of Calgary, Calgary, AB T2N 4N1, Canada
40 Hospital Angeles Tijuana, Tijuana 22010, Mexico
41 Illumina Inc, San Diego, CA 92122, USA
42 Division of Genetics, Department of Pediatrics, UC San Diego School of Medicine, Rady Children's Hospital, San Diego, CA 92123, USA
43 Facultad de Medicina y Psicología, Universidad Autónoma de Baja California, Tijuana 22010, Mexico
44 Breakthrough Genomics Inc, Irvine, CA 92618, USA
45 Department of Pediatrics, University Medical Center Hamburg-Eppendorf, Hamburg 20215, Germany
46 Division of Clinical and Metabolic Genetics, The Hospital for Sick Children, University of Toronto, Toronto, ON M5G 1E8, Canada
47 Fred A Litwin Family Centre in Genetic Medicine, University Health Network and Mount Sinai Hospital, Toronto, ON M5G 2C4, Canada
48 Department of Paediatrics, Hospital for Sick Children and University of Toronto, Toronto, ON M5G 1E8, Canada
49 North East Thames Regional Genetics Service, Great Ormond Street Hospital for Children NHS Foundation Trust, London WC1N 3JH, UK
50 DDC Clinic Center for Special Needs Children, Middlefield, OH 44062, USA
51 Centre de Génétique Humaine, Centre Hospitalier Universitaire, Université de Franche-Comté, Besançon 25000, France
52 UMR 1231 GAD, Inserm, Université de Bourgogne Franche-Comté, Dijon 21000, France
53 Institute of Human Genetics, University Medical Center Hamburg-Eppendorf, Hamburg 20246, Germany
54 Brain and Mitochondrial Research Group, Murdoch Children's Research Institute, Melbourne, Victoria 3052, Australia
55 Pediatric Neurology Unit, Edmond and Lily Safra Children's Hospital, Sheba Medical Center, Ramat Gan 52621, Israel
56 Faculty of Medicine, Tel Aviv University, Tel Aviv 4R73+8Q, Israel
57 Department of Paediatrics, Melbourne Medical School, University of Melbourne, Melbourne, Victoria 3052, Australia
58 Discipline of Genetic Medicine, Sydney Medical School, University of Sydney, Sydney, New South Wales 2050, Australia
59 Discipline of Child and Adolescent Health, Sydney Medical School, University of Sydney, Sydney, NewSouth Wales 2050, Australia
60 Hôpitaux Universitaires de Strasbourg, Laboratoire de Diagnostic Génétique, Strasbourg 67000, France
61 Institute of Human Genetics, Friedrich-Alexander-Universität Erlangen-Nürnberg, Erlangen 91054, Germany
62 Department of Human Genetics, Inselspital Bern, University of Bern, Bern 3010, Switzerland
63 Translational Cytogenomics Research Unit, Bambino Gesù Children's Hospital, IRCCS, Rome 00165, Italy
64 Neurology, Epilepsy and Movement Disorders, Bambino Gesù Children's Hospital, IRCCS, Full Member of European Reference Network EpiCARE, Rome 00165, Italy
65 Department of Medical Genetics, University Hospital of Lyon and Claude Bernard Lyon I University, Lyon 69100, France
66 Pathophysiology and Genetics of Neuron and Muscle (PNMG), UCBL, CNRS UMR5261 - INSERM U1315, Lyon 69100, France
67 Kennedy Center, Department of Clinical Genetics, Copenhagen University Hospital, Rigshospitalet, Copenhagen 2100, Denmark
68 Department of Clinical Medicine, Faculty of Health and Medical Sciences, University of Copenhagen, Copenhagen 2100, Denmark
69 Laboratoires de diagnostic genetique, Institut de genetique Medicale d'Alsace, Hopitaux Universitaires de Strasbourg, Strasbourg 67000, France
70 Center for Rare Diseases, University of Leipzig Medical Center, Leipzig 04103, Germany
71 Guangdong Institute of Intelligence Science and Technology, Zhuhai 519031, China

Correspondence to: Allan Bayat, MD (clinical data)
Department of Epilepsy Genetics and Personalized Medicine, Danish Epilepsy Centre, Dianalund, Denmark
E-mail: abaya@filadelfia.dk

Correspondence may also be addressed to: Yun Stone Shi, PhD (functional evaluation)
Department of Neurology, Nanjing University, Nanjing, China
E-mail: yunshi@nju.edu.cn

Anders Skov Kristensen, PhD (functional evaluation)
Department of Drug Design and Pharmacology, University of Copenhagen, Copenhagen, Denmark
E-mail: ask@sund.ku.dk

Keywords: AMPA receptor; GRIA; GRIA3; clinical biomarker; genotype-phenotype

Introduction

AMPA (α-amino-3-hydroxy-5-methyl-4-isoxazole propionic acid) receptors (AMPARs) belong to the ionotropic glutamate receptor (iGluR) superfamily of ligand-gated cation channels.[1] AMPARs are activated by glutamate (Glu) binding, which triggers the transient opening of a central pore leading to a millisecond influx of cations, denoted excitatory postsynaptic current (EPSC) that depolarizes the postsynaptic membrane and promotes neuronal firing.[2-4] AMPAR-mediated EPSCs are essential components in most excitatory glutamatergic signalling pathways, and normal AMPAR function is critical for most brain functions, including learning and memory formation.[5-13] The assembly of GluA1–A4 subunits into homo- or heterotetrameric receptor complexes forms diverse subtypes of AMPARs with distinct properties and expression patterns.[14,15] The GluA1–4 subunit proteins are highly similar and have a modular architecture of two extracellular domains, the N-terminal domain (NTD) and the agonist binding domain (ABD), a channel-forming transmembrane domain (TMD), and an intracellular carboxy-terminal domain (CTD) of unknown structure (Fig. 1A). The bilobed ABD of each subunit contains a single site where Glu binding initiates conformational changes that are transmitted via semi-flexible linkers to the channel gate in the TMD. Rare genetic variants in the *GRIA1–4* genes[16-21] may disrupt AMPAR physiology and cause developmental and cognitive impairment, behavioural and psychiatric comorbidities, seizures and cerebral malformations.[19,22-56] *GRIA1*, *GRIA2* and *GRIA4* are autosomal genes, whereas *GRIA3* is located on the X-chromosome. While pathogenic missense variants in *GRIA1*, *GRIA2* and *GRIA4* appear to arise almost exclusively *de novo*,[23,25,28] pathogenic variants in *GRIA3* may be transmitted from healthy mothers to affected male children, which is observed in several X-linked neurodevelopmental disorders (NDDs).[27,30]

Currently, 20 *GRIA3* missense variants are reported in 30 patients, of whom four are female.[22,26,27,29-35,38,46-49,55] Of these variants, nine have been functionally tested, revealing or suggesting loss-of-function (LoF) effects for seven variants detected in 15 affected males and in one female[22,29,30,33,35] and gain-of-function (GoF) effects in two variants detected in one female and one male.[32,34] Thus, the phenotypic and genetic landscape in *GRIA3*-related disorders remains ill-defined, lacking genotype-phenotype correlations or clinical biomarkers, particularly in females.

We have therefore systematically interrogated the impact on GluA3-containing AMPAR function of 44 rare inherited or *de novo* *GRIA3* variants identified in patients with NDD to assess these for pathogenicity and establish LoF or GoF effects for overall receptor signalling function. Also, for 25 patients with pathogenic LoF or GoF variants, we compared the clinical features with the functional outcomes to identify genotype-phenotype correlations and clinical biomarkers that could potentially predict the functional outcome of rare *GRIA3* variants. Our results show that *GRIA3*-related disorders encompass two patient groups with distinct clinical features that correlate with the GoF or LoF effect of the variant on receptor function. Also, our findings expand the general knowledge of the pathogenic contribution of rare genetic alterations in *GRIA3* to NDDs in the human population with diverse manifestations, influencing both the timing of disease onset and main clinical symptoms.

Materials and methods

Materials

Unless otherwise stated, all chemicals were from Sigma-Aldrich. Dulbecco's modified Eagle medium (DMEM), fetal bovine serum, trypsin and penicillin-streptomycin were from Invitrogen. DNA-modifying enzymes were from New England Biolabs, except PfuUltra II Fusion HS DNA polymerase. Cyclothiazide (CTZ), kainic acid and 1-naphthyl acetyl spermine (NASPM) were from HelloBio.

Molecular biology

GRIA3 (MIM 138248) variants were introduced by site-directed mutagenesis into their corresponding positions in cDNA expression constructs encoding GluA3. Specifically, the plasmid vectors pXOOF and pCAGGS-IRES-EGFP containing cDNA for the unedited GluA3 flip and flop isoforms ($GluA3_i$ and $GluA3_o$, respectively) were used for heterologous expression in HEK293 cells or generation of mRNA for microinjection in *Xenopus laevis* oocytes (XOs). For pCAGGS-IRES-EGFP, cDNA for $GluA3_i$ and $GluA3_o$ were subcloned into the NheI and XhoI restriction sites of the vector. For pXOOF, the cDNA for $GluA3_i$ was subcloned into the EcoRI and XhoI restriction sites. For co-expression with GluA2, GluA2 was subcloned into the vector pCAGGS-IRES-mCherry. Base pair changes in GluA3 were made by the overlapping PCR method or the QuickChange mutagenesis kit (Stratagene). Genetic changes were verified by Sanger DNA sequencing of the entire GluA3 coding region (GATC Biotech). When used as templates for *in vitro* transcription of mRNA, plasmid constructs were linearized downstream of the 3′ untranslated region using the restriction enzyme NheI, column purified using NucleoSpin DNA clean-up kit (Macherey-Nagel) and stored at a concentration of 1.0 µg/µl at −20°C until use. cRNA transcription was performed using the ARCA mRNA synthesis kit (NEB). The resulting mRNA was purified using the NucleoSpin RNA Clean-up kit (Macherey-Nagel), diluted to 0.5 ng/nl, and stored at −80°C until use.

Xenopus laevis oocyte preparation and injection

Defolliculated XOs (stage V to VI) were prepared and injected with mRNA as previously described.[57] The care and use of *X. laevis*

animals strictly adhered to a protocol (license 2014-15-0201-00031) approved by the Danish Veterinary and Food Administration. Injected XOs were incubated at 18°C in modified Barth's solution (MBS) containing (in mM) 88 NaCl, 1 KCl, 0.41 $CaCl_2$, 2.4 $NaHCO_3$, 0.33 $Ca(NO_3)_2$, 0.82 $MgSO_4$, 5 Tris (pH 7.4) supplemented with 50 µg/ml gentamicin until use. For expression of homomeric GluA3 receptors, XOs were injected with 10 ng cRNA in a volume of 25 nl per oocyte and incubated for 3 days at 18°C in MBS until the experiment. For expression of heteromeric GluA2/A3 receptors, injection of 10 ng of a 2:1 mix ratio of GluA2/GluA3 cRNA was used.

HEK293 cell culturing and transfection

HEK293T cells were cultured in a 37°C incubator with 5% CO_2. Transfection was performed in 35-mm dishes using Lipofectamine 2000 reagents (Invitrogen). For co-expression of GluA3 and GluA2, the ratio of GluA3 to GluA2 cDNA was 1:1. The competitive antagonist NBQX (100 µM) was included in culture media to block receptor-induced cytotoxicity. Twenty-four hours post-transfection, cells were dissociated with 0.05% trypsin, plated on coverslips pre-treated with poly-D-lysine, and used for experiments 4 h after plating.

Electrophysiology

Two-electrode voltage-clamp electrophysiology in *Xenopus laevis* oocytes

Glass micropipettes (0.69 mm ID/1.2 mm OD, Harvard Apparatus) were pulled on a Sutter P-1000 micropipette puller (Sutter Instruments) to a tip resistance of 0.5–2.5 MΩ and filled with 3 M KCl. Oocytes were clamped using a two-electrode voltage-clamp amplifier (OC-725C, Warner Instruments) and continuously perfused with Frog Ringer's solution containing 115 mM NaCl, 2 mM KCl, 5 mM HEPES and 1.8 mM $BaCl_2$ (pH 7.6) by gravity-assisted perfusion at flow rates of 2–4 ml/min into a vertical oocyte flow chamber. Compounds were dissolved in Frog Ringer's solution and added by bath application. Concentration-response data were recorded at holding potentials in the –40 to –80 mV range. Each compound solution was applied for 10–60 s depending on the time needed to obtain steady state currents. Current signals were low-pass filtered at 5 Hz using an USBPGF-S1 programmable instrumentation low-pass filter (Alliagator Technologies) and digitized with a sampling frequency of 10 Hz using a CED 1401plus analogue-digital converter (Cambridge Electronic Design) interfaced with a PC running WinWCP software (available from Strathclyde Electrophysiology Software, University of Strathclyde, Glasgow, UK). Concentration-response experiments were performed by measuring agonist-evoked current during stepwise application of increasing concentrations of agonist, as illustrated in Fig. 1D. All experiments were performed at room temperature.

Whole-cell voltage-clamp electrophysiology in HEK293 cells

The deactivation and desensitization kinetics of glutamate-evoked currents from wild-type (WT) and mutant GluA3 and GluA2/3 receptors were determined in the whole-cell configuration in HEK293 cells. After the formation of whole-cell configuration, individual HEK293 cells were lifted with 3–5 MΩ borosilicate glass pipettes filled with the following internal solution: 135 mM KF, 33 mM KOH, 2 mM $MgCl_2$, 1 mM $CaCl_2$, 11 mM EGTA, 10 mM HEPES (pH 7.2). Glu (10 mM) was dissolved in the extracellular solution: 140 mM NaCl, 2.5 mM KCl, 2 mM $CaCl_2$, 1 mM $MgCl_2$, 10 mM HEPES, 5 mM glucose (pH 7.2). Glutamate pulses of 1 or 500 ms were applied to cells using a theta-glass pipette mounted on a piezoelectric bimorph driven by gravity. Glutamate-induced currents were recorded using a MultiClamp 700B amplifier (Axon Instruments) with membrane potential held at –70 mV. Current signals were recorded with an Axon Digidata 1440 data acquisition system and with a sampling frequency of 100 kHz following low-pass filtration over 2 kHz. All experiments were performed at room temperature.

Cohort

Patients with inherited or *de novo* *GRIA3* variants were recruited through an international collaboration with epilepsy and NDD research groups, the Leipzig GRI-registry (https://www.uniklinikum-leipzig.de/einrichtungen/humangenetik/Seiten/GRI-registry.aspx), Decipher,[58] ClinVar[59] and via GeneMatcher.[60] We also contacted the healthcare providers of previously published patients to collect new or updated clinical information or used that previously reported in the literature[26,29,33,34,61] (seven patients). Clinical information was collected by the local physicians or caregivers and included data on the age of seizure onset and offset, seizure semiology, developmental trajectory, medical history, physical examination, EEG and neuroimaging. The study was conducted in agreement with the Declaration of Helsinki. The Leipzig GRI-registry was approved by the local ethical committee; Leipzig/Germany (224/16-ek and 379/21-ek). As all probands were minors or had cognitive impairment, their parents or legal guardians provided written informed consent.

Data and statistical analysis

Data for concentration-response curves were obtained from analysis of electrophysiological recordings of agonist-evoked current responses using ClampFit 10 software (Molecular Devices). Current responses were normalized to the current response by maximal agonist concentration and used to construct composite concentration-response plots from at least eight oocytes and fitted using GraphPad Prism v9 (GraphPad Software, San Diego, CA, USA) to a four-variable Hill equation:

$$response = bottom + \frac{top - bottom}{1 + 10^{(logEC_{50} - X) \times nH}} \quad (1)$$

where *bottom* is the fitted minimum response, *top* is the fitted maximum response, *nH* is the Hill slope, *X* is the agonist concentration, and EC_{50} is the half-maximally effective agonist concentration, respectively. The time constants for the rate of desensitization (τ_{desens}) and deactivation (τ_{deact}) were obtained by fitting current responses evoked by 500 and 1 ms Glu pulses with an exponential function using a non-linear least square algorithm (ClampFit):

$$I = I1 \times \left(\exp\left(-\frac{time}{\tau 1}\right)\right) + I2 \times \left(\exp\left(-\frac{time}{\tau 2}\right)\right) \quad (2)$$

where *I* is the total current amplitude, *I*1 and *I*2 are the amplitudes of the fast and slow current components, respectively, and τ1 and τ2 are the time constants for the decay of the fast and slow current components. The weighted average τ was then calculated as follows:

$$\tau_{weighted} = \left(\frac{I1 \times \tau 1 + I2 \times \tau 2}{I1 + I2}\right) \quad (3)$$

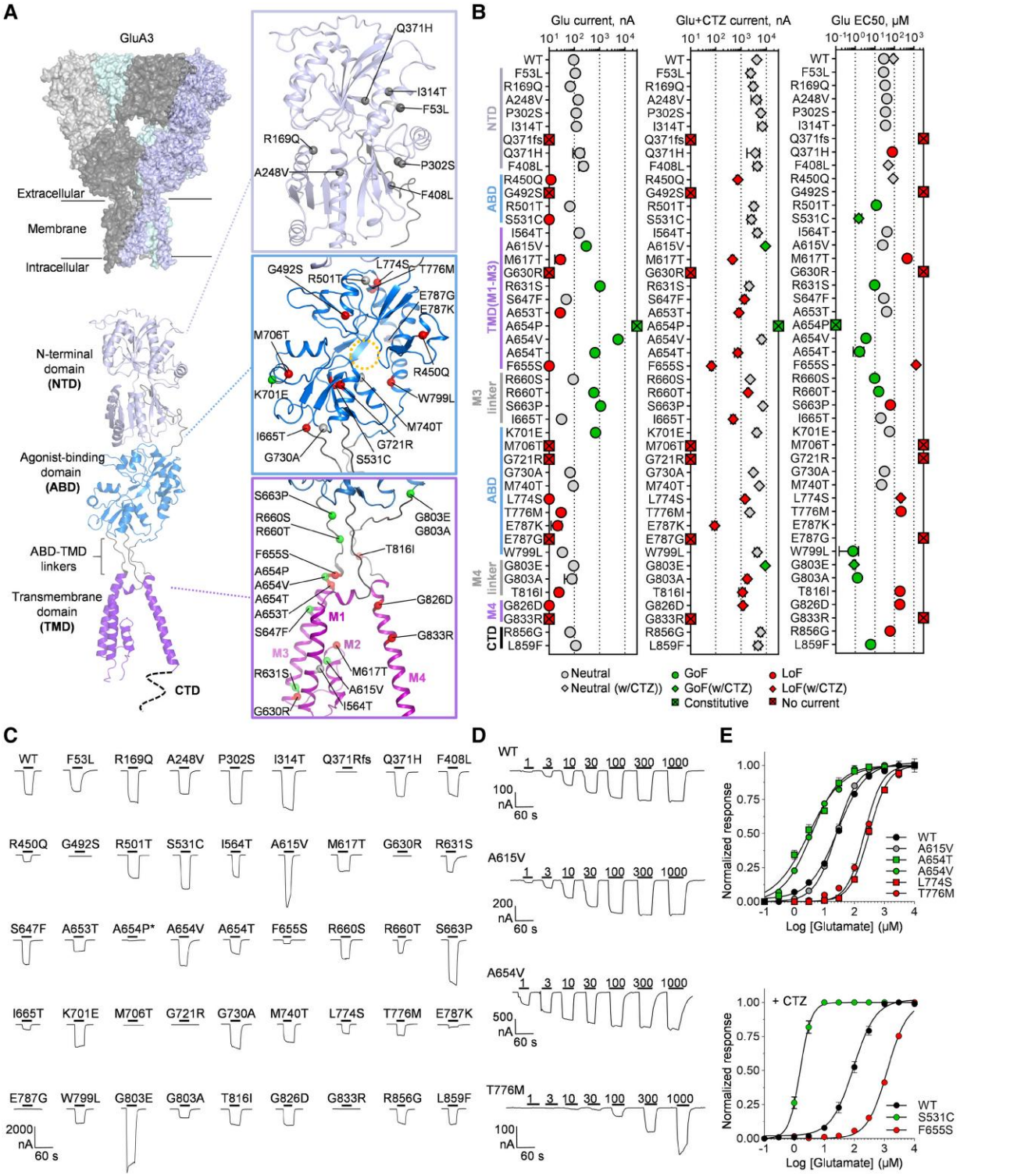

Figure 1 Location of *GRIA3* variants in the GluA3 receptor and effect on glutamate-gated channel function. (**A**) Structural model of homomeric GluA3 receptor encoded by the *GRIA3* gene built from structures of the GluA2 receptor (Supplementary material, 'Materials and methods' section). The *top left* panel shows a surface representation of the tetrameric receptor complex with the four identical subunits. The *bottom* panel shows a cartoon representation of a single GluA3 subunit with the N-terminal domain (NTD), the agonist-binding domain (ABD), and the transmembrane domain (TMD). Zoomed views of the NTD, ABD and TMD show the position of genetic variants caused by *GRIA3* missense variants highlighted by different colours according to the apparent effect on homomeric GluA3 function as neutral, loss-of-function (LoF) and gain-of-function (GoF). The stippled circle indicates the position of the Glu binding site in the ABD. (**B**) Summary of desensitized (Glu) and non-desensitized (Glu + CTZ) current amplitudes and Glu EC50 for homomeric GluA3 receptors containing genetic variants encoded by the *GRIA3* variants evaluated in this study. Values, number of measurements, and statistical parameters are given in Supplementary Tables 2 and 3. Individual data-points are colour-coded according to the effect on currents or EC50 (LoF effect) or increase (GoF effect). For the EC50 panel, data-points shown as squares represent EC50 values determined with

(continued)

All desensitization time constants were determined using the two-component fitting and τ_{desens} is reported as the weighted average τ. Unless otherwise stated, all deactivation time constants were determined using mono-exponential fitting, using Eq. 2 with *I2* fixed at 0. Statistical analyses of data were performed in GraphPad Prism 9. Unless otherwise stated, summary patch-clamp and two-electrode voltage-clamp (TEVC) electrophysiology data are represented as mean with a 95% confidence interval (CI). One-way ANOVA with Dunnett's *post hoc* multiple comparison test was performed for comparisons of three or more groups in which the data were normally distributed and where a *P*-value <0.05 was considered significant. For statistical analysis of clinical data, quantitative statistics were analysed using SPSS software (version 24, IBM, UK). Two-sided T-test was used to determine the association of clinical features with the LoF and GoF patient groups. *P*-value < 0.05 was considered significant. Unless otherwise stated, the level of statistical significance is denoted as $^{*}P < 0.05$, $^{**}P < 0.01$ and $^{***}P < 0.001$. Extended statistical information including specific *P*-values are provided in the Supplementary material.

Results

GRIA3 missense variants concentrate on domains responsible for glutamate binding and channel gating

To investigate the pathogenicity of *GRIA3* variants identified in NDD patients, we collected one frameshift variant and 43 *GRIA3* missense variants identified in patients with presumed *GRIA3*-related NDD (see the 'Materials and methods' section) (Fig. 1 and Supplementary Table 1). Notably, although the central elements for channel function (the ABD, TMD and ABD-TMD linkers) constitute <50% of the GluA3 subunit protein, the majority of the *GRIA3* missense variants are located in the ABD (15 variants) and TMD (13 variants) domains, and the ABD-TMD linkers (six variants). In addition, none of these 34/43 variants are reported in the Genome Aggregation Database (gnomAD) and *GRIA3* is predicted to be constrained to missense variants ($Z = 4.23$), which indicates intolerance to missense variation and the majority are predicted to be damaging by *in silico* prediction of deleteriousness (Supplementary Table 1). In contrast, only nine variants affect residues in the NTD and CTD, which are non-critical domains for the core ligand-gated channel function (Fig. 1A and Supplementary Table 1).

GRIA3 variants have gain-of-function or loss-of-function effects on GluA3 receptor function

The majority of the identified *GRIA3* missense variants have not been functionally evaluated for effects on GluA3-containing AMPAR function, except for variants p.(Arg450Glu), p.(Ala615Val), p.(Arg631Ser), p.(Ala653Thr), p.(Arg660Thr), p.(Met706Thr), p.(Glu787Gly), p.(Glu787Lys), p.(Gly826Asp) and p.(Gly833Arg),[22,29,30,32-35] although not in a systematic manner. Therefore, we first evaluated all variants with TEVC electrophysiology to directly compare effects, focusing on key receptor functional features that included current amplitude, Glu sensitivity, receptor activation and desensitization properties (Fig. 1B and C). Specifically, *GRIA3* variants were introduced in cDNA encoding GluA3 and expressed in XOs as homomeric receptors. We first recorded current responses following the application of a single high Glu concentration (300 µM) with pharmacological blockade of receptor desensitization (Fig. 1C). Twenty of the variants showed currents that were significantly lower than wild-type, including nine variants with undetectable or very small (e.g. 50-fold lower than wild-type) current amplitude (Fig. 1B and C and Supplementary Table 2), indicating that these variants have severe LoF effects on GluA3 subunit function or expression. The single frameshift variant p.(Gln371Argfs*6) is located in the 5′ end of the NTD-encoding segment of the *GRIA3* coding sequence (Fig. 1A). Therefore, this variant results in the expression of only the NTD that cannot form a functional receptor. Indeed, the expression of p.(Gln371Argfs*6) in XOs did not yield any current response (Fig. 1C) and is assigned a complete LoF status. The remaining variants produced current responses with amplitudes similar to or within 2-fold range of wild-type (Fig. 1B and C and Supplementary Table 2), except for the variants p.(Ala615Val), p.(Ser663Pro) and p.(Gly803Glu), which showed more than 2-fold significantly increased currents compared to wild-type, suggesting an overall GoF effect on receptor function.

For all functional variants, we performed dose-response experiments with increasing concentrations of Glu (Fig. 1D) and determined the half-maximally effective concentration (EC_{50}) for receptor activation (Fig. 1E, Supplementary Fig. 2 and Supplementary Table 3). As summarized in Fig. 1B, 20 variants changed the EC_{50} significantly by more than 2-fold. The most pronounced changes were observed for the p.(Ser531Cys), p.(Ala654Thr), p.(Trp799Leu) and p.(Gly803Ala) variants, which decreased EC_{50} more than 20-fold (considered a GoF effect) and p.(Met617Thr) and p.(Phe655Ser), which increased EC_{50} by more than 20-fold (considered a LoF effect) (Fig. 1B and E, Supplementary Fig. 2 and Supplementary Table 3).

AMPARs undergo profound desensitization in the continued presence of Glu, which is a key property for EPSC shape and protects against excitotoxicity due to glutamatergic hyperfunction.[1,62,63] For variants with a residual function, we assessed potential effects on receptor desensitization by recording consecutive Glu currents in the absence (I_{GLU}) and presence (I_{GLU+TZ}) of CTZ block of desensitization (Fig. 2A). The wild-type GluA3 receptor showed desensitized current amplitude of $2.8 \pm 0.4\%$, $n = 79$, of the non-desensitized current amplitude (Fig. 2A and B and Supplementary Table 3); corresponding well with previously reported ratios for homomeric GluA3.[64-66] Eight variants displayed significant increases in the desensitized current as illustrated for a representative variant [p.(Ala654Val)] in Fig. 2A. The variants p.(Arg631Ser), p.(Ala654Pro), p.(Ala654Val) and p.(Ala654Thr) showed the most profound effects, with near identical current amplitudes under desensitizing and non-desensitizing conditions (Fig. 2A and B and Supplementary Table 3), which indicate that the variants decrease or fully block receptor desensitization, which is a GoF effect for AMPAR signalling. In contrast, seven variants [p.(Ser531Cys, p.(Leu774Ser), p.(Thr776Met), p.(Trp799Leu), p.(Gly803Ala), p.(Thr816Ile), p.(Gly826Asp)] significantly decreased

Figure 1 (Continued)
cyclothiazide (CTZ). (**C**) Representative current responses from two-electrode voltage-clamp (TEVC) recordings of *Xenopus laevis* oocytes (XOs) (V_{HOLD} −40 mV) expressing wild-type (WT) or *GRIA3* variant-containing GluA3 receptors in response to Glu application (300 µM, black bar) in the presence of CTZ (100 µM) to block desensitization. (**D**) Representative current recordings from TEVC Glu concentration-response experiments of wild-type GluA3 and selected variants exemplifying neutral [p.(Ala615Val)], increasing [p.(Ala654Val)] or decreasing [p.(Thr776Met)] effect on receptor responsiveness to Glu. (**E**) Composite concentration-response curves for wild-type and selected *GRIA3* variant-containing GluA3 receptors. Data-points represent the mean of 6–12 oocytes. Error bars are the standard error of the mean (SEM) and are shown when larger than the symbol size. The current responses are normalized to the maximal response evoked by Glu. In all panels, variants are labelled with single-letter amino acid codes.

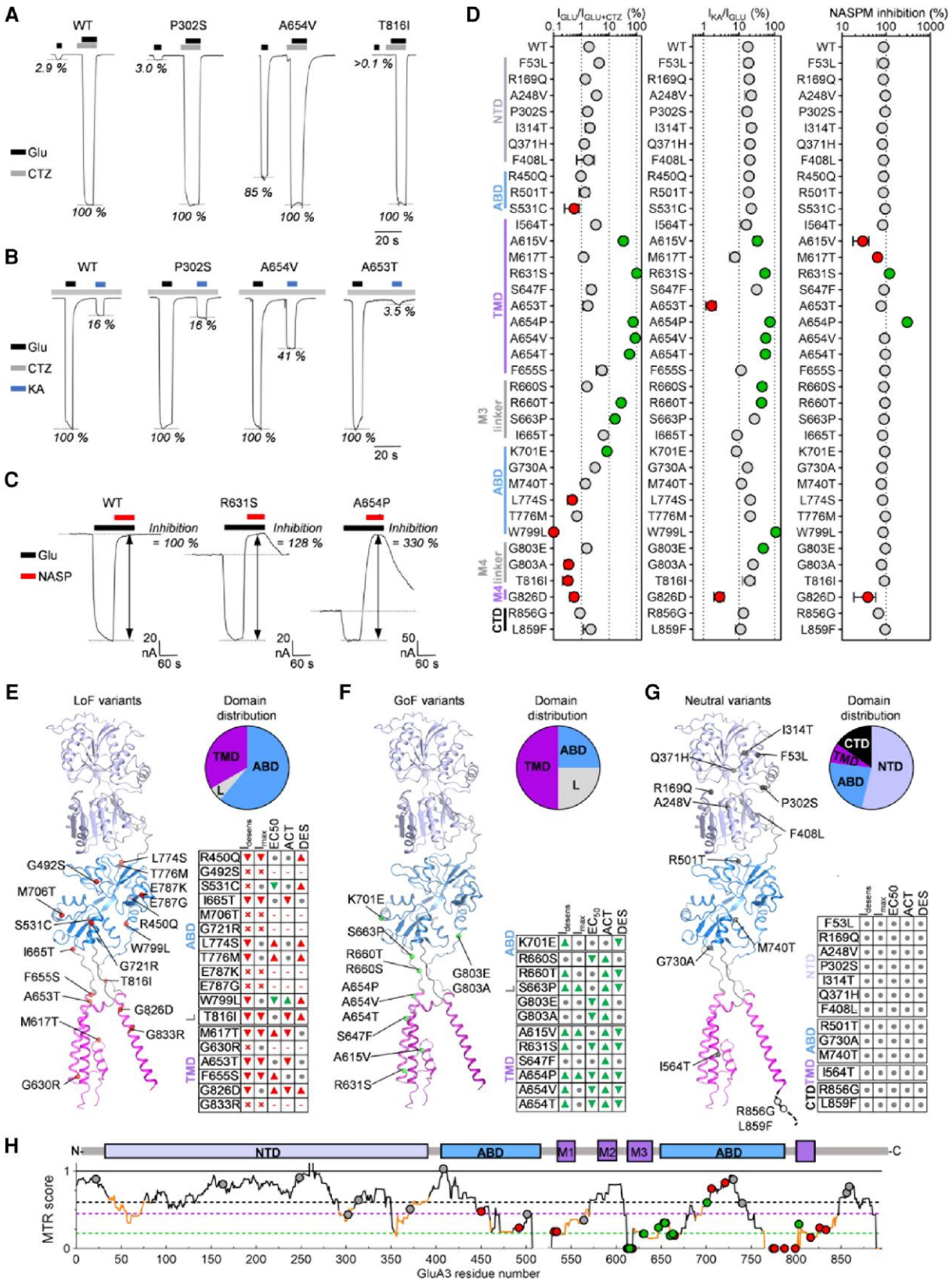

Figure 2 Variant effects on receptor desensitization and activation properties. (**A**) Representative currents evoked by sequential 10–20 s applications of Glu (1 mM, black bar) alone and in the presence of cyclothiazide (CTZ) (100 μM, grey bar) from oocytes expressing wild-type (WT) GluA3 and GluA3 carrying selected *GRIA3* missense variants. The p.(Pro302Ser) variant shows no change in the size of the desensitized current relative to the non-desensitized Glu current compared to wild-type, the p.(Ala654Val) variant shows increased desensitized current, and the p.(Thr816Ile) variant show decreased desensitized current. (**B**) Representative currents evoked by sequential 10–20 s applications of Glu (1 mM, black bar) and kainic acid (KA)

(continued)

the desensitized current relative to the non-desensitized current, indicating an increase in receptor desensitization, which is considered a LoF effect (Fig. 2B and Supplementary Table 3).

We screened for changes in the activation properties of GluA3, comparing the receptor current evoked by application of the weak partial agonist kainic acid (KA) versus the current evoked by Glu[68,69] (Fig. 2C). When desensitization was blocked, the KA current (I_{KA+CTZ}) at wild-type GluA3 was 21 ± 0.1%, $n = 85$, of the Glu current (Fig. 2B and Supplementary Table 3). The results from the screening showed an increased KA efficacy for 12 variants [p. (Ala615Val), p.(Arg631Ser), p.(Ser647Phe), p.(Ala654Pro), p.(Ala654Val), p.(Ala654Thr), p.(Arg660Ser), p.(Arg660Thr), p.(Ser663Pro), p.(Trp799Leu), p.(Gly803Glu) and p.(Gly803Ala) (Fig. 2C and Supplementary Table 3). This effect indicates an increase in the ability of GluA3 to translate agonist binding to channel opening and is to be considered a GoF effect for overall receptor function. In contrast, six variants [p.(Met617Thr), p.(Ala653Thr), p.(Phe655Ser), p.(Ile665Thr), p.(Lys701Glu) and p.(Gly826Asp)] displayed decreased KA efficacy and, therefore, reduced ability to activate, which is a LoF effect for overall receptor function (Fig. 2B and C and Supplementary Table 3). Notably, the KA/Glu current ratio has previously been electrophysiologically characterized for homomeric GluA3 with the p.(Ala653Thr) variant with similar results.[29]

Last, we screened for constitutive receptor activity, e.g. channel opening in the absence of Glu, using NASPM, a selective open-channel blocker for GluA2-lacking calcium-permeable AMPARs.[70,71] Applying 1 μM NASPM produced near-complete inhibition of the Glu-evoked current for wild-type GluA3 and most variants (Fig. 2C and D and Supplementary Table 3). However, for two variants [p.(Arg631Ser) and p.(Ala654Pro)], NASPM application inhibited the membrane current below the level observed in the absence of Glu (Fig. 2C), indicating constitutive channel activity. This effect was most profound for the variant p.(Ala654Pro) (Fig. 2D and Supplementary Table 3). Specifically, in the absence of an agonist and at a holding potential of −40 mV, XOs expressing the p.(Ala654Pro) variant displayed ∼10-fold increased membrane current (564 ± 123 nA; $n = 21$) compared to XOs expressing the wild-type (receptor 61 ± 32 nA; $n = 20$). Also, the elevated membrane current for p.(Ala654Pro) increased relatively little upon Glu application in the presence of block of desensitization ($I_{GLU+CTZ}$ = 89 ± 20 nA; $n = 18$) compared to the membrane current in wild-type expressing ($I_{GLU+CTZ}$ = 4230 ±490 nA; $n = 140$), but decreased by >300% upon NASPM application (Fig. 2D and Supplementary Table 3). Three variants [p.(Ala615Val), p.(Met617Thr) and p.(Gly826Asp)] showed decreased inhibition by NASPM. These variants change residues located close to the NASPM binding site in the channel, and the decreased inhibition by NASPM likely reflects a direct effect on the binding affinity of NASPM.[72]

The TEVC functional characterizations of the 43 missense *GRIA3* variants showed that 70% (30/43) changed one or more of the evaluated receptor parameters. As summarized in Fig. 2E, 18 of the missense variants showed a pattern of functional effects that point to an overall LoF effect on receptor signalling function, including decreased or complete loss of desensitized and non-desensitized current response to Glu (no or decreased I_{GLU} or $I_{GLU+CTZ}$, respectively), reduced agonist sensitivity (increased EC_{50}), reduced activation ability (decreased I_{KA}/I_{GLU} ratio) or increased desensitization (decreased $I_{GLU}/I_{GLU+CTZ}$ ratio). In contrast, 12 variants showed effect patterns that suggest an overall GoF effect; e.g. increased current amplitudes, agonist sensitivity, activation, including constitutive activity and significantly reduced or completely blocked desensitization (Fig. 2F). Two variants [p.(Trp799Leu) and p.(Ser531Cys)] showed a mixed pattern of both GoF and LoF effects. Specifically, these variants showed no [p.(Ser531Cys)] or greatly reduced [p.(Trp799Leu)] desensitized current, but wild-type-like current amplitude upon block of desensitization (Fig. 1B and C and Supplementary Tables 2 and 3). These results suggest a LoF functional phenotype due to increased desensitization. On the other hand, both variants decreased Glu EC_{50} dramatically (Fig. 1E; measured in the presence of CTZ), which is a GoF effect, and for p.(Trp799Leu) also increased the KA efficacy, indicating increased ability to be activated (Fig. 1B and Supplementary Table 3). However, we classified both variants to have an overall LoF effect based on the reduced Glu current without blocked desensitization. Last, 13 variants did not show significant changes in any of the evaluated functional parameters (Fig. 2G) and, therefore, appeared neutral for the core ligand-gated channel function and were not investigated further. However, we cannot rule out that these variants may affect other aspects of GluA3-containing receptors beyond the functions studied here, such as receptor trafficking, regulation and interactions with synaptic proteins important for native AMPARs.

The domain distribution of the GoF, LoF and functionally neutral variants shows that GoF and LoF variants exclusively affect residues in the ABD, TMD and ABD-TMD linkers, whereas most neutral variants affect residues in the NTD and CTD (Fig. 2E–G). Overall, the positions in the GluA3 sequence that are affected by LoF and GoF

Figure 2 (Continued)
(300 μM; blue bars) in the presence of CTZ (100 μM, grey bar) from oocytes expressing wild-type GluA3 and GluA3 containing selected variants exemplifying different types of variant effects on KA/GLU response ratio. For wild-type GluA3 and the p.(Pro302Ser) variant, the KA-evoked current has an amplitude of 16% of the Glu current amplitude. In contrast, the p.(Ala654Val) variant has a relative KA current of 41%, indicating an increase in activation properties, and p.(Ala653Thr) variant has decreased relative KA response amplitude of 3.5%, indicating decreased activation properties. The holding potential was −40 mV in all shown recordings. (**C**) Representative currents illustrating 1-naphthyl acetyl spermine (NASPM) (1 μM, red bar) inhibition of Glu-evoked currents for wild-type GluA3 and GluA3 containing the variants p.(Arg631Ser) and p.(Ala654Pro). (**D**) Summary of the ratio of desensitized and non-desensitized current amplitude ($I_{GLU}/I_{GLU+CTZ}$), non-desensitized Glu and KA ($I_{KA+CTZ}/I_{GLU+CTZ}$) current amplitudes and NASPM inhibition of Glu-evoked current for homomeric GluA3 receptors containing genetic variants encoded by the *GRIA3* variants evaluated in this study. Values, number of measurements and statistical parameters are given in Supplementary Table 2. Individual data-points are colour-coded according to the effect on currents or EC_{50} [loss-of-function (LoF) effect; red] or increase [gain-of-function (GoF) effect; green]. (**E–G**) Summary of phenotype and domain location of variants with overall GoF (**E**), LoF (**F**) and neutral (**G**) effect on homomeric GluA3 receptor function. Inverted triangle = decrease; triangle = increase; filled circle = no change; dash = not determined. Colour-coding indicates a predicted LoF (red) or GoF (green) effect of change on overall receptor function. (**H**) Missense tolerance ratio (MTR) of *GRIA3* variants analysed with a 31 amino acid window calculated using the MTR-viewer online tool (https://biosig.lab.uq.edu.au/mtr-viewer/).[67] A line graph displays the MTR distribution for *GRIA3* (gene transcript NM_000828) with regions in orange indicating observed variation differs significantly from neutrality. Dashed lines on the plot denote gene-specific MTRs: green = fifth percentile; purple = 25th percentile; black = 50th percentile. Above the MTR distribution is shown the domain structure of the GluA3 subunit. Variant positions are shown as circles on the MTR line graph and coloured according to functional effect as: neutral (grey), GoF (green) and LoF (red). Orange line segments indicate regions where the observed variation differs significantly from neutrality. In all panels, variants are labelled with single-letter amino acid codes. ABD = agonist binding domain; CTD = carboxy-terminal domain; NTD = N-terminal domain; TMD = transmembrane domain.

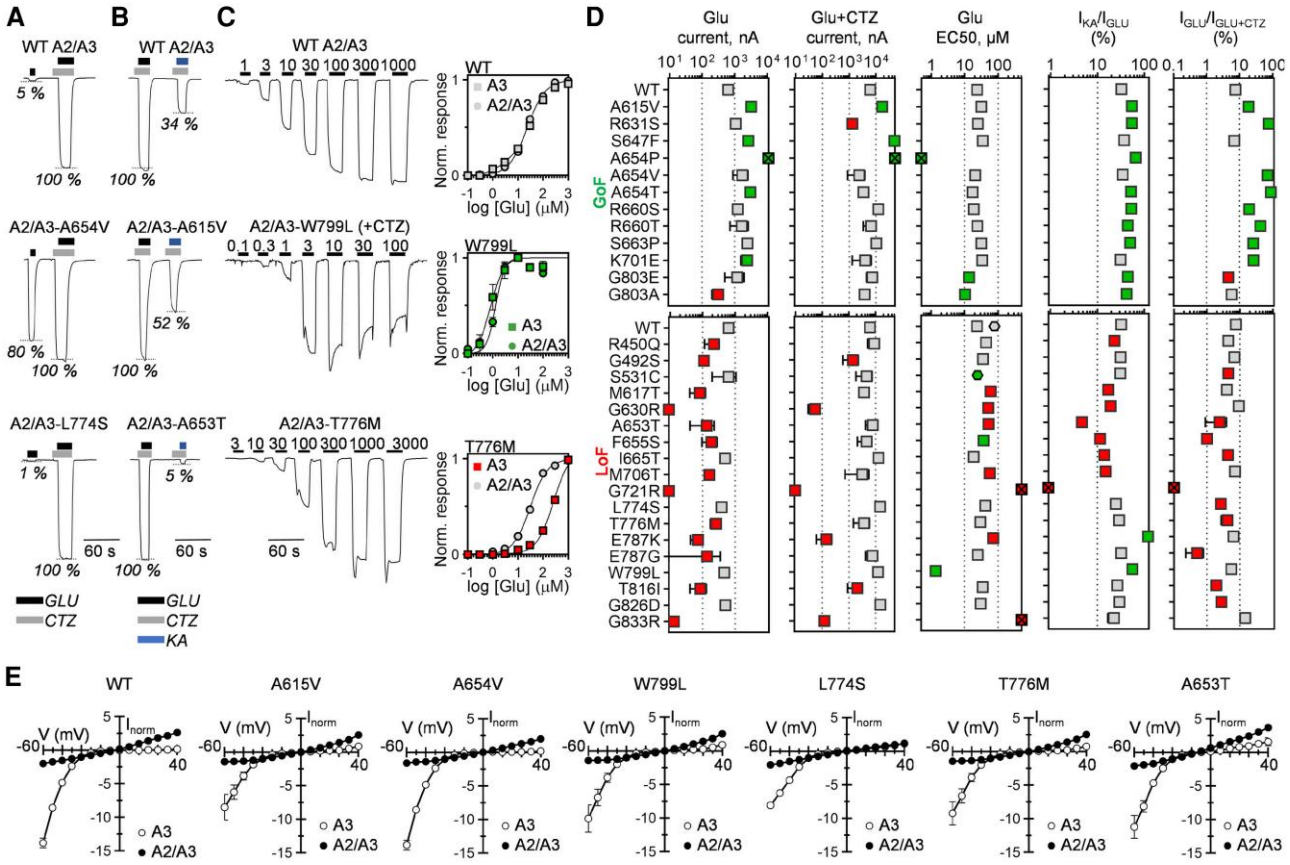

Figure 3 Variant effects in heteromeric GluA2/A3 receptors. (**A**) Representative currents evoked by sequential 10–20 s applications of Glu (1 mM) alone and in the presence of cyclothiazide (CTZ) (100 μM) from oocytes expressing wild-type (WT) GluA2, wild-type GluA3 and wild-type GluA2 with GluA3 carrying selected *GRIA3* missense variants illustrating increased [p.(Ala654Val), middle trace] and decreased [p.(Leu774Ser); lower trace] desensitized current. (**B**) Representative currents evoked by sequential 10–20 s applications of Glu (1 mM) and kainic acid (KA) (300 μM) the presence of CTZ (100 μM) from oocytes expressing wild-type GluA2, wild-type GluA3 and wild-type GluA2 with GluA3 carrying selected *GRIA3* missense variants illustrating increased [p.(Ala615Val), middle trace] and decreased [p.(Ala653Thr); lower trace] current response to KA relative to Glu. (**C**) Representative current recordings from two-electrode voltage-clamp (TEVC) Glu concentration-response experiments of wild-type and selected variants in heteromeric GluA2/A3 receptors with corresponding fitted dose-response curves for homomeric (A3) and heteromeric (A2/A3) receptors. The p.(Trp799Leu) exemplifies a variant changing the EC_{50} in both homomeric and heteromeric receptors, whereas p.(Thr776Met) exemplifies a variant affecting only homomeric receptors. (**D**) Overview and summary of the effects on heteromeric GluA2/A3 receptor parameters (squares) of *GRIA3* variants with gain-of-function (GoF) and loss-of-function (LoF) effects. Data-points represent the mean and 95% confidence interval (CI) values (Supplementary Tables 2 and 3). (**E**) Current-voltage (IV) relationships of Glu-evoked currents from oocytes expressing homomeric wild-type and variant-containing GluA3 alone and with wild-type GluA2R. The current amplitude at the different holding potentials is normalized to the current at −40 mV. Data-points represent the mean from 6 to 10 oocytes. Error bars indicate the standard error of the mean (SEM) and are shown when larger than the symbol size. In all panels, variants are labelled with single-letter amino acid codes.

variants fit well with analysis of missense tolerance ratio[73] (MTR) (Fig. 2H), as 87% (27/31) of the variants with functional LoF or GoF affect residues in segments that appear highly intolerant to missense variation (Fig. 2H), whereas 69% (9/13) of the functionally neutral variants affect positions with no unusual sensitivity to missense variation. This observation suggests that MTR analysis is a highly effective predictor of potential pathogenicity of missense variants for *GRIA3*. In comparison, the accuracy of the *in silico* prediction tools SIFT and PolyPhen in predicting the LoF/GoF variants as pathogenic was 72% and 74%, respectively (Supplementary Table 1).

GRIA3 variant effects are dominant in heteromeric AMPA receptors

GluA3 subunits are thought to preferentially assemble with GluA2 subunits into heteromeric GluA2/3 receptors in the brain, although triheteromeric GluA1/2/3 receptors have also recently been shown.[74-77] Thus, native GluA3-containing AMPARs in affected patients will have two subunits containing the variant. To assess whether variant effects were also present in heteromeric GluA2/A3 receptors, we expressed the LoF or GoF variants together with wild-type GluA2 and determined desensitized and non-desensitized current amplitudes, the degree of desensitization, and the KA/GLU response ratio (Fig. 3A–C and Supplementary Table 4). For each variant expressed with GluA2, the current-voltage (IV) relationship was determined, as this provides a measure for formation of heteromeric GluA2/A3 receptors (Fig. 3E). Specifically, incorporation of GluA2 subunits shifts the IV curve from inwardly-rectifying to linear (as illustrated for wild-type and selected variants in Fig. 3E). All functional variants exhibited linear IV relationships when expressed with GluA2, which shows that the variants retain their ability of GluA3 to form heteromeric GluA2/A3 receptors. As summarized in Fig. 3D, the results showed

that GoF effects observed in homomeric GluA3 were highly penetrant to heteromeric GluA2/A3. Specifically, significant changes for the affected parameters were also observed in GluA2/A3 receptors for all variants exhibiting one or more GoF effects. Similarly, for variants that induced a LoF phenotype for homomeric GluA3, LoF effects were also observed in the heteromeric receptor background. Notably, among the variants that completely abolished the Glu response in homomeric GluA3 [p.(Gly492Ser), p.(Gly630Arg), p.(Met706Thr), p.(Gly721Arg), p.(Glu787Lys), p.(Glu787Gly) and p.(Gly833Arg)], currents could be measured for all when expressed as heteromers with GluA2, although with profoundly lower current amplitudes than wild-type GluA2/A3 (Fig. 3D and Supplementary Table 2). The only exception was the p.(Gly721Arg) variant, which showed a current amplitude similar to wild-type in heteromeric GluA2/A3 receptors (Supplementary Table 2). For all of these variants, a linear IV relationship similar to wild-type GluA2/3 was observed (Supplementary Fig. 3), confirming the presence of the GluA2 subunit in the heteromeric receptor complex.

In summary, the characterization of the effects of the 43 *GRIA3* missense variants revealed 31 (72%) to alter electrophysiological functions in both homomeric GluA3 and heteromeric GluA2/3 receptors, strongly indicating these variants as pathogenic.

Kinetic characterization and classification of the pathogenic variants

Based on the TEVC evaluations, we next aimed to collect detailed phenotypic and genetic information from patients carrying the 31 *GRIA3* variants associated with significant LoF or GoF effects on receptor function and, therefore, are strongly indicated as a monogenetic cause of NDD. For 17 of these variants, we obtained detailed clinical information from 25 NDD patients, resulting in a cohort of 14 males (Patients M1–M14) and 11 females (Patients F1–F11). The genetic and phenotypic details of the patient cohort are described in the Supplementary material and Supplementary Table 7. To further characterize how the 17 cohort variants perturb the receptor functional phenotype, we utilized fast-application patch-clamp electrophysiology, which can model the synaptic Glu pulses that evoke EPSCs on a millisecond timescale and can accurately identify changes in receptor deactivation and desensitization rates that are particularly important for shaping AMPAR synaptic signals. Specifically, the cohort variants were expressed in HEK293 cells as homomeric GluA3 and heteromeric GluA2/A3 receptors. Current responses to pulses of 10 mM Glu were recorded (Fig. 4A for an illustration of the recording protocol and representative current traces), except for variants p.(Ala653Thr), p.(Gly630Arg) and p.(Arg660Thr), which have previously been characterized with fast-application patch-clamp electrophysiology in both homomeric GluA3 and heteromeric GluA2/A3 receptors.[29,34,61] AMPAR subunits occur in two isoforms, denoted flip and flop, which result from alternative splicing of the two mutually exclusive exons, 14 and 15, respectively, and have important differences in receptor kinetics.[78] This alternative flip/flop splicing affects nine amino acid positions in a 38 amino acid segment close to the ABD-M4 linker. The p.(Glu787Gly) (Patient M7), p.(Glu787Lys) (Patient M8–9 and F11) and p.(Trp799Leu) (Patient F9) variants originate in exon 14 and specifically affect the flop isoform. Therefore, these variants were characterized in the flop isoform of GluA3 ($GluA3_o$). The remaining variants are located outside the flip/flop segment and were characterized in the flip isoform ($GluA3_i$), which predominates before birth and continues to be expressed in the adult brain.[79]

The results showed a complete or very severe LoF effect on the current response to fast Glu applications for the variants p.(Gly492Ser) (Patient M2), p.(Phe655Ser) (Patient M10), p.(Ile665Thr) (Patient F10) and p.(Glu787Gly) (Patient M7) (Fig. 4A). In addition, the variants p.(Gly630Arg) (Patients M3–6) and p.(Glu787Lys) (Patients M8–9 and F11) that previously have been characterized with identical recording protocols, also have a complete LoF phenotype.[61] Moreover, expressed together with wild-type GluA2, all these variants also abolished the current response in heteromeric GluA2/A3 receptors, except for p.(Ile665Thr) (Patient F10), which showed a robust and desensitizing current response (Fig. 4A). To test whether the complete or severe LoF effect was due to the variants perturbing expression and folding of the GluA3 subunit protein, or subunit ability to assemble into receptors that traffic to the membrane, we expressed β-lac-tagged wild-type and variant GluA3 constructs in HEK293 cells (Supplementary material, 'Methods' section). Analysis of the conversion rates of the β-lac substrate nitrocefin from transfected HEK293 cells revealed no significant difference in cell-surface expression between wild-type and variant receptors (Supplementary Fig. 4). Thus, we conclude that the LoF effect that these variants have on Glu current is due to disruption of the core ligand-gated channel function of the receptor. The p.(Trp799Leu) variant showed measurable currents but with greatly reduced peak amplitude. In homomeric GluA3, due to the reduced currents, we were only able to reliably determine the desensitization rate of the p.(Trp799Leu) variant in a single experiment, which showed 3-fold increased rate of desensitization (τ_{des} = 0.57 ms versus 1.58 ± 0.05 ms; n = 15 for wild-type $GluA3_o$) and no measurable steady-state current (Fig. 4A and B and Supplementary Table 5). These effects were also observed in the heteromeric GluA2/A3 receptor (Fig. 4A and B and Supplementary Table 5), where slightly more robust currents allowed us to accurately determine the desensitization kinetics, and suggest p.(Trp799Leu) is a severe LoF variant by greatly reducing charge transfer due to an increased rate and extent of receptor desensitization. Notably, this is supported by the TEVC characterizations that showed that the diminished Glu current for p.(Trp799Leu) could be fully rescued by the pharmacological block of desensitization (Figs 2 and 3).

The GoF variants p.(Ala654Val), p.(Ala654Thr), p.(Ala654Pro), p.(Ser663Pro), p.(Lys701Glu), p.(Gly803Ala) and p.(Gly803Glu) all produced robust currents when expressed as homomeric and heteromeric receptors (Fig. 4A). For these variants we determined the desensitization rate (τ_{des}) and peak-to-steady-state current ratio (I_{ss}) from 500 ms lutamate stimulations (Fig. 4B and C) and the deactivation rate (τ_{deact}) from 1 ms stimulations (Fig. 4D and E and Supplementary Table 5). As predicted from the TEVC results, p.(Ala654Val) (Patient F5), p.(Ala654Thr) (Patient F7) and p.(Ala654Pro) (Patient F6) displayed greatly decreased desensitization. Specifically, whereas wild-type $GluA3_i$ currents almost completely decayed within milliseconds (τ_{des} = 5.3 ± 0.3 ms; n = 12) to a small fraction of the peak current (I_{ss} = 1.1 ± 0.1%; n = 16), the p.(Ala654Pro) variant completely blocked (I_{ss} = 100 ± 0.0%, n = 4) and the p.(Ala654Thr) and p.(Ala654Val) variants greatly reduced the level of desensitization (I_{ss} = 82 ± 3%, n = 9, and 61 ± 2%, n = 9, respectively). In addition, the deactivation rates for these variants were also slowed (τ_{deact} = 5–22 ms; n = 3–9) compared to wild-type (τ_{deact} = 2.1 ± 0.2 ms; n = 9) for homomeric GluA3 receptors (Fig. 4D and E and Supplementary Table 5). These effects were maintained for the heteromeric GluA2/A3 receptor, where the p.(Ala654Pro) variant completely blocked desensitization and slowed deactivation, and the p.(Ala654Val) and p.(Ala654Thr) decreased desensitization and

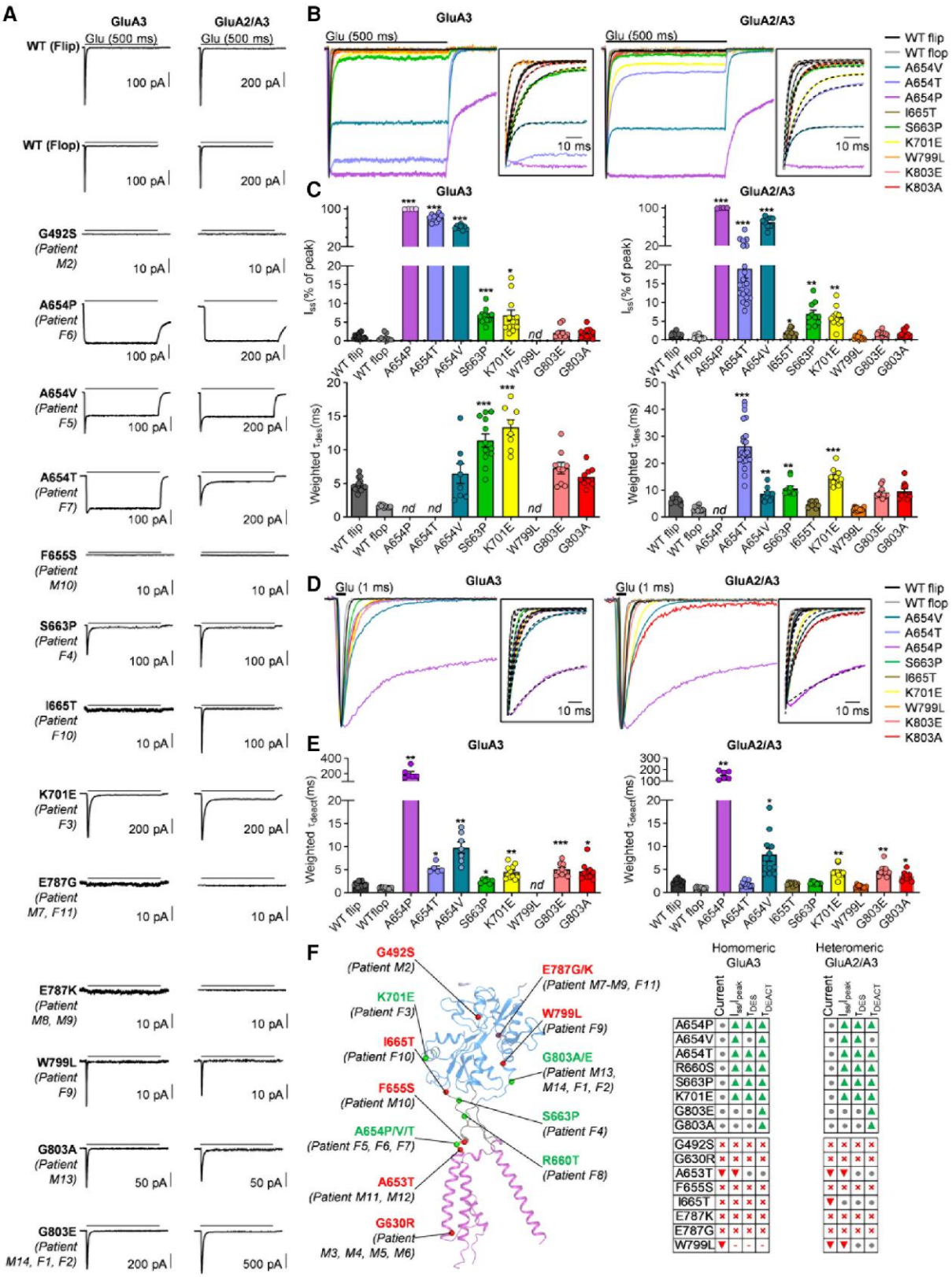

Figure 4 Characterization of variant effect on fast receptor kinetics. (**A**) Representative whole-cell currents evoked by a 500 ms application of glutamate (Glu) (10 mM, black bar) from homomeric GluA3 (*left*) and heteromeric GluA2/A3 receptors carrying the indicated *GRIA3* variants subunits expressed in HEK293 cells. The holding potential was −70 mV in all recordings. Note that scale bars for current amplitude differ between recordings. (**B**) The time constant (τ_{des}) and level (I_{ss}) of current desensitization determined from the fitting of the current decay (*insert*) during 500 ms applications of Glu (10 mM, black bars) fitted to two-exponential decay functions weighted by proportional contributions for wild-type (WT) and variant homomeric

(continued)

slowed deactivation, except for p.(Ala654Val), which showed a deactivation rate not different from wild-type (Fig. 4B and C and Supplementary Table 5). Thus, the three variants affecting Ala654 can be classified as severe GoF due to profoundly decreased desensitization and reduced deactivation rates. The variants p.(Ser663Pro) (Patient F4) and p.(Lys701Glu) (Patient F3) displayed phenotypes quite similar to each other, which included significantly increased I_{ss} levels, slowed desensitization rates and modestly but significantly slowed deactivation rates in both homomeric and heteromeric receptors (Fig. 4B and C and Supplementary Table 5). Lastly, the two variants affecting Gly803 [p.(Gly803Ala) and p.(Gly803Glu)] showed normal I_{ss} levels but reduced desensitization and deactivation rates (Fig. 4B and C and Supplementary Table 5). These changes, as a consequence of p.(Ser663Pro), p.(Lys701Glu), p.(Gly803Ala) and p.(Gly803Glu) variants, are predicted to have a clear GoF effect on the synaptic charge carried by GluA3-containing AMPARs, although to a less severe extent than the variants affecting Ala654.

Correlation of loss-of-function and gain-of-function receptor effects with patient clinical phenotype

We next compared patient clinical information with the receptor phenotypic information. As summarized in Fig. 5A, we classified the variants based on the GoF and LoF effects identified in the electrophysiological analyses as severe or mild. In addition, data from previously reported evaluations of the p.(Ala653Thr)[29] and p.(Arg660Thr)[34] variants were included. For LoF variants, the severe class includes seven variants in 12 patients (Patients M1–M10 and F10–F11; Fig. 5A) that completely abolish the current response to millisecond Glu stimulation, whereas the mild class includes two variants from three patients [p.(Ala653Thr) in Patients M11 and M12 and p.(Trp799Leu) in Patient F9], which show current response to fast Glu stimulation, but with greatly reduced amplitude and profound changes in desensitization and deactivation kinetics that overall are predicted to reduce synaptic charge transfer. For GoF variants, the mild class includes four patients with variants p.(Gly803Ala) (Patient M13) and p.(Gly803Glu) (Patients M14 and F1 and F2), which slow desensitization and deactivation rates significantly increase Glu sensitivity, but do not appear to change peak or desensitized current levels. The severe GoF class includes the variants p.(Ala654Val), p.(Ala654Pro) and p.(Ala654Thr) (Patients F5–F7), respectively, in addition to p.(Ser663Pro) (Patient F4), p.(Arg660Thr) (Patient F8) and p.(Lys701Glu) (Patient F3), which all significantly reduce desensitization and deactivation rates, increase Glu sensitivity and increase steady state current amplitudes in the TEVC experiments (Fig. 5A).

Several differences between the GoF and LoF patient classes (10 patients with GoF variants and 15 patients with LoF variants) were identified (Table 1 and Fig. 5B). Importantly, LoF and GoF variants are disease-causing in both sexes but affected males predominantly (12/14) carry hemizygous LoF variants. In contrast, most affected females (8/11) carry heterozygous GoF variants. Another striking difference includes the age of seizure onset in the subgroup of patients with epileptic comorbidities, muscle tone (hypo- versus hypertonia), sleep difficulties and movement disorders, including hyperekplexia (Fig. 5B and Table 1). Specifically, for the patients with epileptic comorbidities, the median age of seizure onset in patients harbouring a GoF was 1 month (range first day to 12 months, $n = 5$), being significantly earlier than in patients with LoF variants, being 16.5 months (range 12–36 months, $n = 6$, $P = 0.004$). We detected no significant differences between the GoF and LoF groups when comparing seizure types ($P = 0.85$) and treatment response ($P = 1$). For body tone, most patients harbouring a LoF variant had congenital muscular hypotonia ($n = 10/15$), which was not reported in any of the 10 patients with GoF variants ($P = 0.0004$). In contrast, congenital muscular hypertonia was present in 8/10 patients with GoF variants, while it was only reported in 1/15 patients with LoF variants ($P = 0.0002$). Sleep disturbances were reported in 10/15 patients with LoF variants, while they were only present in 2/10 patients with GoF variants ($P = 0.0018$). Movement disorders of any kind were reported in 5/15 patients with LoF variants, while they were present in 8/10 patients with a GoF variant ($P = 0.04$). In particular, an excessive startle response to external stimuli, also known as hyperekplexia, was more prevalent in the group with GoF variants ($n = 5$) compared to the group with LoF variants ($n = 1$) ($P = 0.003$). For behavioural abnormalities, aggressive outbursts were more prevalent in the LoF cohort ($n = 6$) compared to the GoF cohort ($n = 2$), although the difference was not significant ($P = 0.29$). There were no significant differences in the other behavioural abnormalities reported in the GoF ($n = 6$) compared to the LoF cohort ($n = 10$) ($P = 0.75$). Although all patients had intellectual disability (ID), we found no significant difference in severity between the GoF and LoF cohorts ($P = 0.26$). Specifically, ID was reported to be borderline/mildly ($n = 1$), moderately ($n = 5$), severely ($n = 8$) or profoundly ($n = 1$) affected in the LoF cohort, while moderately ($n = 4$), severely ($n = 3$) or profoundly ($n = 3$) affected in the GoF cohort.

In summary, the phenotypic assessment indicates that GoF variants are objectively associated with more severe outcomes: patients were younger at the time of seizure onset, hypertonic and more often had movement disorders, including hyperekplexia. In contrast, patients with LoF variants were older at seizure onset, hypotonic and had sleep difficulties.

Discussion

Missense variants in *GRIA3* are by far the most prevalently reported *GRIA* genetic defects in NDD patients. However, the extent to which the variants underlie NDDs is not clear, as few have been studied in cellular or animal models to confirm them as pathogenic variations. The present work systematically evaluates 44 rare *GRIA3* variants in NDD patients to establish whether these have functional effects on GluA3-containing AMPARs. Focusing on effects on core ligand-gated ion channel function, we found that 31 variants produced significant effects and were classified as LoF or GoF concerning overall receptor signalling capability. We correlated the identified effects on receptor function with the clinical features and found distinct GoF and LoF phenotypes. This specific LoF-GoF

Figure 4 (Continued)
GluA3 (*left*) and heteromeric GluA2/A3 (*right*) receptors. (**C**) Summary of the τ_{des} and I_{ss} values. Bars represent the mean with standard error of the mean (SEM) error. Values not determined due to low or no current are labelled 'nd'. (**D**) Deactivation rates (τ_{deact}) determined from the fitting of the current decay (*insert*) following 1 ms application of Glu (10 mM, black bars) fitted to a mono-exponential decay function (*inserts*) for wild-type and variant homomeric GluA3 (*left*) and heteromeric GluA2/A3 (*right*) receptors. (**E**) Summary of τ_{deact} values. Bars represent the mean with SEM error. Values not determined due to low or no current are labelled 'nd'. (**F**) Summary of effects of patient variants on current kinetics and location in GluA3 subunit. Variants with loss-of-function (LoF) effects are shown in red and gain-of-function (GoF) in green. Inverted triangle = decrease; triangle = increase; filled circle = no change; dash = not determined. In all panels, variants are labelled with single-letter amino acid codes.

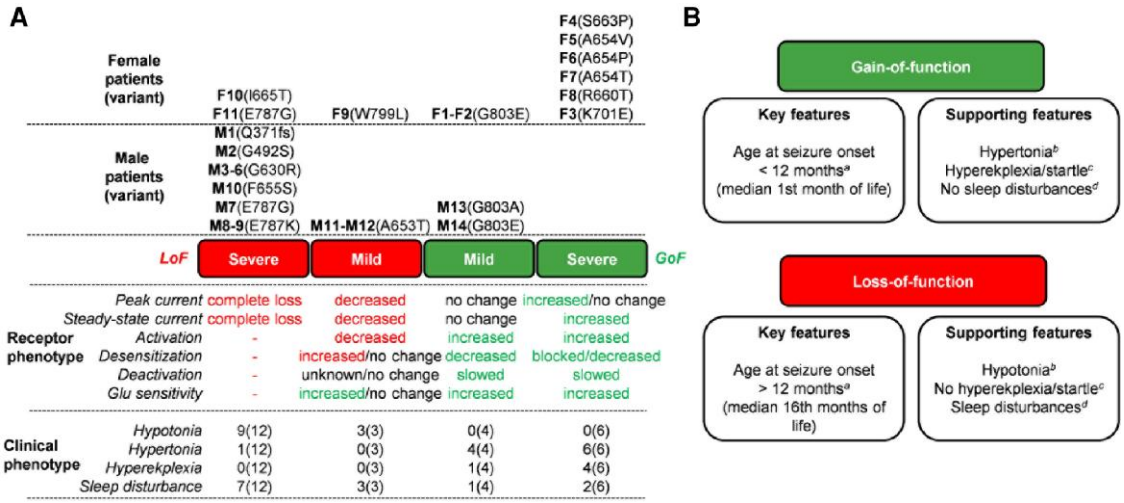

Figure 5 Variant classification and phenotype correlations for Patients M1–M14 and F1–F11. (**A**) Schematic overview of the classification of receptor phenotype for Patients M1–M14 and F1–F11 into severe and mild gain-of-function (GoF; green) and loss-of-function (LoF; red) categories based on variant effect patterns on GluA3-containing receptor function together with an overview of the number of patients and prevalence of key patient symptoms for each category. (**B**) Summary of key and supporting features for the clinical phenotypes associated with LoF and GoF variants. The diagram summarizes several clinical findings that can help predict if a *GRIA3* variant leads to LoF and GoF. GoF variants manifest with seizures occurring before the first year of life (with a median age of 1 month) and are characterized by supporting features such as hypertonia, hyperekplexia/excessive startle reflex, and the absence of sleep disturbances. LoF variants manifest with key features such as seizure onset after the first year of life (with a median age of 16 months) and supporting features including hypotonia, sleep disturbances and the absence of hyperekplexia/excessive startle reflex. If a patient's phenotypical presentation displays a combination of these features, functional testing of the variant is required to determine whether a *GRIA3* variant displays LoF or GoF characteristics. [a–d]*P*-values for comparing proportions of clinical indicators between the LoF or GoF patients. [a]Age of seizure onset 12 months; $P = 0.004$. [b]Hypertonia versus hypotonia; $P = 0.0004$. [c]Hyperekplexia/startle versus no hyperekplexia/startle; $P = 0.003$. [d]Sleep disturbance versus no sleep disturbance; $P = 0.018$.

difference in clinical phenotype is in line with several other CNS ion channel gene families, including the *GRIN* iGluR gene subfamily,[80] where studies applying detailed electrophysiological analysis of rare missense variant effects have established both LoF and GoF effects as pathogenic, with each category often leading to different disease phenotypes.[81-86] In addition to the clinical importance of providing a diagnosis and new disease understanding, identifying pathogenic variants as having LoF or GoF effects on channel function is also of therapeutic relevance as it potentially guides pharmacological intervention. For the iGluR gene families, this approach of systematic and detailed testing of pathogenic variants from patient cohorts and their clinical and therapeutic relevance has been successfully implemented for the NMDAR-encoding *GRIN* gene family, leading to a definition of specific neurological conditions associated with types of variant effect and examples of successful therapeutic intervention.[1,87,88] In this paper, we extend the value of this approach to the *GRIA* family. Moreover, our data advance the understanding of the role of abnormal function of AMPARs in general and GluA3-containing subtypes in particular in NDD syndromes. First, as 71% of the evaluated variants altered GluA3-containing AMPAR function, *GRIA3* can be firmly classified as a general disease gene in NDDs, and underscores the importance of appropriate AMPAR signalling for CNS development, as also suggested in single case or smaller cohort studies for *GRIA1*, *GRIA2* and *GRIA3*.[22,29,30,32-34] Second, our work expands the spectrum and frequency of functional effects of pathogenic *GRIA3* variants by identifying distinct types of LoF and GoF effects and providing clear genotype-phenotype correlations that define two clinical phenotypes associated with predicted LoF and GoF effects: LoF variants often lead to muscular hypotonia, hyporeflexia, a sleep disorder, aggressive behaviour and later onset of seizures, whereas GoF variants are associated with muscular hypertonia, hyperreflexia, startle-induced non-epileptic myoclonia and earlier onset of seizures.

Although the GoF variants appear to be associated with more severe outcomes, such as earlier seizure onset and a higher prevalence of movement disorders, including hyperekplexia, all patients present with overall severe NDD phenotypes independent of the type of LoF or GoF effect of the *GRIA3* variants. This observation suggests that even quantitatively small alterations from wild-type AMPAR function lead to severe outcomes, which likely reflects the crucial role of AMPARs in the ability of excitatory synapses to detect transmission events rapidly. As excitatory synaptic currents can occur at rates of up to several hundred Hz, AMPARs have likely evolved with precisely balanced Glu sensitivity and extremely fast rates of activation, desensitization and deactivation within a very narrow range. Thus, although some LoF and all GoF effects do not prevent the contribution of GluA3-containing AMPARs to synaptic transmission, they are likely to perturb the fidelity of neuronal activation. It is also noteworthy that Patient M1, who is hemizygous for the protein-truncating complete LoF variant p.(Gln371Argfs*6), appears to have the least severe symptoms compared to those with missense LoF variants, in particular in respect to the severity of ID (Table 1). This finding suggests that the complete loss of GluA3-containing receptors from synaptic AMPAR populations is better tolerated than the existence of GluA3-containing receptors with perturbed function. Interestingly, similar findings have been reported for γ-aminobutyric acid A ($GABA_A$) receptors.[89] Further detailed evaluation of more pathogenic *GRIA3* variants is warranted to explore how clinical severity correlates to variant effects on receptor function and will likely require establishing models for studying the

Table 1 Comparison of clinical features reported in patients with loss-of-function *GRIA3* variants compared to features reported in those with gain-of-function *GRIA3* variants

Feature	Loss-of-function	Gain-of-function
Number of patients	15	10
Male	12/15 (80%)	2/10 (20%)
Female	3/15 (20%)	8/10 (80%)
Epilepsy diagnosis	6/15 (40%)	6/10 (60%)
Median age at onset of seizures	16 months (range 9 months to 3 years)	1 month (range first day to 27 years)
Treatment resistant seizures	3/5 (60%)	4/6 (66%)
Developmental delay or cognitive impairment	15/15 (100%)	10/10 (100%)
	Degree: borderline = 1 mild-moderate = 1 moderate = 4 severe = 7 severe-profound = 1 profound = 1	Degree: moderate = 4 severe = 2 severe-profound = 1 profound = 3
Muscular hypotonia	12/15 (80%)	0/10 (0%)
Muscular hypertonia	2/15 (13%)	9/10 (90%)
Hyporeflexia	10/15 (66%)	0/10 (0%)
Hyper-reflexes	1/15 (6%)	7/10 (70%)
Spasticity	1/15 (6%)	4/10 (40%)
Movement disorder or any kind	7/15 (46%)	8/10 (80%)
Hyperexplexia or stimulus sensitive non-epilepticus myoclonia	2/15 (13%)	6/10 (60%)
Sleep disorder	10/15 (66%)	3/10 (33%)
Behavioural issues of any kind	10/15 (66%)	5/10 (50%)
Aggressive outburst or self-damaging behaviour	6/15 (40%)	2/10 (20%)
MRI performed	9/15 (60%)	9/10 (90%)
Abnormal MRI	2/9 (22%)	2/9 (22%)

The table summarizes key clinical features in the loss-of-function and gain-of-function patient groups. Detailed clinical information for individual patients is provided in the Supplementary material and Supplementary Table 7.

variant impact on synaptic transmission and animal behavioural phenotypes.

The current dataset also provides insight into emerging associations among sex and inheritance, which often is complicated for morbid genes on the X-chromosome, as it is not always possible to predict the phenotypical effect in heterozygous females. Our dataset establishes that LoF and GoF variants as disease-causing, but that affected males more often (12/14) carry hemizygous LoF variants, whereas most affected females (8/11) carry heterozygous GoF variants. Although our data do not support a strict model, the prevalence of *de novo* GoF in females is consistent with the general understanding that LoF variants are likely to be less harmful in heterozygous females.[90] However, evaluation of further *GRIA3* variants in males and females is needed to explore (i) the prevalence of GoF variants in females and LoF variants in males; and (ii) to describe if males with GoF variants are equally or more severely affected than females with similar variants.

Next-generation sequencing has become routine in hospitals and the number of NDD patients with a genetic aetiology is increasing.[91,92] As a result, the number of new *GRIA* variants needing a functional assessment is expected to rise. In addition to confirming pathogenicity, functional testing provides knowledge crucial for treatment, as choosing the right drug (effective and not exacerbating the existing symptoms) depends on establishing LoF or GoF status. In this respect, establishing the impact of new variants on AMPAR function via electrophysiological evaluation may become a critical bottleneck in individual cases, highlighting a need to develop approaches for the theoretical prediction of variant pathogenicity and LoF/GoF effects. Notably, recent large-scale bioinformatical efforts for exploring new approaches for prediction of pathogenicity of variants in genes encoding voltage- and ligand-gated ion channel subunits have suggested that clinical decision support algorithms that predict LoF/GoF status based on location in protein structure may become feasible.[93] Specifically, it was shown that certain positional measures of the variant in the structures of voltage-gated sodium channels and NMDA receptors could be correlated to functional effect and clinical phenotype.[93] For similar purpose in GluA3-containing AMPA receptors, we note that when considering the variant distribution throughout the GluA3 structure, it is observed that functionally neutral variants are enriched in the NTD, whereas LoF or GoF variants localize in the ABD, linker and TMD segments (Figs 1 and 2). However, we found several examples of close clustering of neutral, LoF and GoF variants in these domains, which suggests that the clinical interpretation of missense variants in *GRIA3* as well as GoF/LoF classifications based on general localization measures in the receptor structure should be cautious.

For several pathogenic *GRIA3* variants, our analysis allows us to pinpoint the mechanistic cause of the overall LoF or GoF effect. This knowledge provides an opportunity for exploring clinically relevant AMPAR drugs for the pharmacological rescue of receptor function among different classes of variant phenotypes. Notably, for variants with LoF effects on AMPAR kinetics, positive allosteric modulators (PAMs) exist, in particular of the ampakine class, that can modulate AMPAR current amplitude and waveform via selective effects on receptor kinetics.[94] Although no AMPAR PAM currently is FDA/EMA approved, several have passed phase I/II clinical trials, such as CX516,[95] CX717 (fasoracetam),[96] Org 24448 (aniracetam)[97] and CX1739,[98] including early proof-of-concept trials in patients with cognitive impairments[99] and are subjects for ongoing clinical development. Similarly, for variants with GoF effects (e.g. increased activation or decreased desensitization), negative allosteric modulators (NAMs) can be explored, including perampanel, which inhibits activation and accelerates desensitization.[100] Importantly, perampanel is approved for chronic treatment of several types of epilepsy[101] and therefore, directly available as a potential precision medicine for patients with GoF AMPAR mutations, as recently has been demonstrated for GoF variants in other *GRIA* genes.[102]

The present study represents the largest functional evaluation of missense variants in any *GRIA* gene. Together with previous work on *GRIA1*, *GRIA2* and *GRIA3*, the volume of validated pathogenic *GRIA* variants has now reached a critical point that firmly establishes *GRIA* genetic defects as the cause of an emerging neurological disease, recently referred to as *GRIA* disorder.[102] However, further understanding of *GRIA* disorder disease mechanisms and potentially devising standard rescue pharmacological strategies is complicated by the diversity of the native AMPAR subtypes that a pathogenic variant can affect. Notably, we focused our functional work on the homomeric GluA3 and the heteromeric GluA2/A3 subtypes in two heterologous expression models, which

lack the postsynaptic proteins that interact with native AMPARs and contribute to their synaptic functions. Most native AMPARs assemble with different transmembrane AMPA receptor regulatory proteins (TARPs), which act as auxiliary subunits and have distinct effects on receptor function, including modulation of receptor gating and desensitization properties.[1,103] These effects may have significant implications for the variant effect on synaptic transmission, and further work is required to provide insights into how *GRIA* variants affect AMPAR function involving auxiliary subunits. Also, the absence of a neuronal environment presents a caveat to the classification of variants that do not display functional effects, as functionally neutral variants may have detrimental effects on other aspects of AMPAR cellular biology, such as receptor incorporation and positioning at synapses and regulation during synaptic plasticity mechanisms. Specifically, our evaluation did not reveal effects on the core function of GluA3-containing AMPARs for 13 variants when evaluated in recombinant GluA3 receptors (Fig. 1). Recent progress in mapping the AMPAR interactome in the brain shows that native AMPARs during the receptor lifetime interact with more than 40 intracellular, extracellular or membrane-embedded proteins, which are important for proper receptor biogenesis, postsynaptic positioning and function.[104] We cannot rule out that apparently neutral variants may indeed influence expression and function of native GluA3-constaining AMPARs by interfering with the ability of the GluA3 subunit to interact with synaptic constituents, and confident classification of *GRIA3* variants as neutral is thus not possible in current practice. Therefore, studies beyond establishing the functional defects of *GRIA* variants are needed to describe effects in a synaptic context. Importantly, the impact of LoF/GoF variants on the AMPAR-component of EPSC currents should be determined and correlated with the effects on kinetic parameters obtained from heterologous expression systems. This will improve the framework of predicting synaptic effects for variants based on functional evaluations in reduced systems such as XOs or HEK293 cells.

We have characterized the consequences of 44 *GRIA3* variants identified in NDD patients on GluA3-containing receptor function. Although the spectrum of variant effects on AMPAR signalling mechanisms that underlie the phenotype of each patient is likely to be complex, our analysis shows two significant genotype-phenotype correlations that correspond to predicted GoF or LoF effects on the signalling function of GluA3-containing AMPARs.

Data availability

The authors confirm that the data supporting the findings of this study are available in the main text and its Supplementary material.

Acknowledgements

We thank the families for participating in this study. This study makes use of data generated by the DECIPHER community. A full list of centres that contributed to the generation of the data is available from https://deciphergenomics.org/about/stats and via e-mail from contact@deciphergenomics.org. In addition, we thank the ERN EPICARE network for promoting our collaborative call on *GRIA*-related disorders. This work has been generated within the European Reference Network on Rare Congenital Malformations and Rare Intellectual Disability (ERN-ITHACA) [EU Framework Partnership Agreement ID: 3HP-HP-FPA ERN-01-2016/739516].

Funding

Funding for the DECIPHER project was provided by Wellcome [grant number WT223718/Z/21/Z]. This work has been generated within the European Reference Network on Rare Congenital Malformations and Rare Intellectual Disability (ERN-ITHACA) [EU Framework Partnership Agreement ID: 3HP-HP-FPA ERN-01-2016/739516]. A.B. is funded by Novo Nordisk Foundation BRIDGE Programme (NNF20SA0064340). J.H.S. is supported by the National Natural Science Foundation of China (32200779). The research conducted at the Murdoch Children's Research Institute (MCRI) was supported by the Victorian Government's Operational Infrastructure Support Program. The Royal Children's Hospital Foundation generously supports the Chair in Genomic Medicine awarded to J.C. L.C.B. is supported by the National Institutes of Health (5U54OD030165). Y.S.S. is supported by the National Key Research and Development Program of China (2019YFA0801603), the National Natural Science Foundation of China (32170951), the Fundamental Research Funds for the Central Universities (021414380533) and Special Fund for Science and Technology Innovation Strategy of Guangdong Province (2021B0909050004). A.S.K. is supported by Independent Research Fund Denmark (3101-00386B).

Competing interests

The authors report no competing interests.

Supplementary material

Supplementary material is available at *Brain* online.

References

1. Hansen KB, Wollmuth LP, Bowie D, et al. Structure, function, and pharmacology of glutamate receptor ion channels. *Pharmacol Rev*. 2021;73:298-487.
2. Raman IM, Trussell LO. The kinetics of the response to glutamate and kainate in neurons of the avian cochlear nucleus. *Neuron*. 1992;9:173-186.
3. Sah P, Hestrin S, Nicoll RA. Properties of excitatory postsynaptic currents recorded in vitro from rat hippocampal interneurones. *J Physiol*. 1990;430:605-616.
4. Silver RA, Traynelis SF, Cull-Candy SG. Rapid-time-course miniature and evoked excitatory currents at cerebellar synapses in situ. *Nature*. 1992;355:163-166.
5. Hayashi Y, Shi SH, Esteban JA, Piccini A, Poncer JC, Malinow R. Driving AMPA receptors into synapses by LTP and CaMKII: Requirement for GluR1 and PDZ domain interaction. *Science*. 2000;287:2262 LP-2262267.
6. Barria A, Muller D, Derkach V, Griffith LC, Soderling TR. Regulatory phosphorylation of AMPA-type glutamate receptors by CaM-KII during long-term potentiation. *Science*. 1997;276:2042-2045.
7. Kauer JA, Malenka RC, Nicoll RA. A persistent postsynaptic modification mediates long-term potentiation in the hippocampus. *Neuron*. 1988;1:911-917.
8. Mahanty NK, Sah P. Calcium-permeable AMPA receptors mediate long-term potentiation in interneurons in the amygdala. *Nature*. 1998;394:683-687.
9. Rumpel S, LeDoux J, Zador A, Malinow R. Postsynaptic receptor trafficking underlying a form of associative learning. *Science*. 2005;308:83-88.

10. Lee HK, Takamiya K, Han JS, et al. Phosphorylation of the AMPA receptor GluR1 subunit is required for synaptic plasticity and retention of spatial memory. *Cell*. 2003;112:631-643.
11. Esteban JA, Shi SH, Wilson C, Nuriya M, Huganir RL, Malinow R. PKA phosphorylation of AMPA receptor subunits controls synaptic trafficking underlying plasticity. *Nat Neurosci*. 2003;6:136-143.
12. Hu H, Real E, Takamiya K, et al. Emotion enhances learning via norepinephrine regulation of AMPA-receptor trafficking. *Cell*. 2007;131:160-173.
13. Kessels HW, Malinow R. Synaptic AMPA receptor plasticity and behavior. *Neuron*. 2009;61:340-350.
14. Schwenk J, Baehrens D, Haupt A, et al. Regional diversity and developmental dynamics of the AMPA-receptor proteome in the mammalian brain. *Neuron*. 2014;84:41-54.
15. Swanson GT, Kamboj SK, Cull-Candy SG. Single-channel properties of recombinant AMPA receptors depend on RNA editing, splice variation, and subunit composition. *J Neurosci*. 1997;17:58-69.
16. Keinänen K, Wisden W, Sommer B, et al. A family of AMPA-selective glutamate receptors. *Science*. 1990;249:556-560.
17. Puckett C, Gomez CM, Korenberg JR, et al. Molecular cloning and chromosomal localization of one of the human glutamate receptor genes. *Proc Natl Acad Sci U S A*. 1991;88:7557-7561.
18. Sun W, Ferrer-Montiel AV, Schinder AF, McPherson JP, Evans GA, Montal M. Molecular cloning, chromosomal mapping, and functional expression of human brain glutamate receptors. *Proc Natl Acad Sci U S A*. 1992;89:1443-1447.
19. Gécz J, Barnett S, Liu J, et al. Characterization of the human glutamate receptor subunit 3 gene (GRIA3), a candidate for bipolar disorder and nonspecific X-linked mental retardation. *Genomics*. 1999;62:356-368.
20. Boulter J, Hollmann M, O'Shea-Greenfield A, et al. Molecular cloning and functional expression of glutamate receptor subunit genes. *Science*. 1990;249:1033-1037.
21. Hollmann M, O'Shea-Greenfield A, Rogers SW, Heinemann S. Cloning by functional expression of a member of the glutamate receptor family. *Nature*. 1989;342:643-648.
22. Piard J, Béreau M, XiangWei W, et al. The GRIA3 c.2477G > A variant causes an exaggerated startle reflex, chorea, and multifocal myoclonus. *Mov Disord*. 2020;35:1224-1232.
23. Geisheker MR, Heymann G, Wang T, et al. Hotspots of missense mutation identify neurodevelopmental disorder genes and functional domains. *Nat Neurosci*. 2017;20:1043-1051.
24. Hackmann K, Matko S, Gerlach EM, et al. Partial deletion of GLRB and GRIA2 in a patient with intellectual disability. *Eur J Hum Genet*. 2013;21:112-114.
25. Salpietro V, Dixon CL, Guo H, et al. AMPA receptor GluA2 subunit defects are a cause of neurodevelopmental disorders. *Nat Commun*. 2019;10:3094.
26. Trivisano M, Santarone ME, Micalizzi A, et al. GRIA3 missense mutation is cause of an x-linked developmental and epileptic encephalopathy. *Seizure*. 2020;82:1-6.
27. Philips AK, Sirén A, Avela K, et al. X-exome sequencing in Finnish families with intellectual disability—four novel mutations and two novel syndromic phenotypes. *Orphanet J Rare Dis*. 2014;9:49.
28. Martin S, Chamberlin A, Shinde DN, et al. De novo variants in GRIA4 lead to intellectual disability with or without seizures and gait abnormalities. *Am J Hum Genet*. 2017;101:1013-1020.
29. Davies B, Brown LA, Cais O, et al. A point mutation in the ion conduction pore of AMPA receptor GRIA3 causes dramatically perturbed sleep patterns as well as intellectual disability. *Hum Mol Genet*. 2017;26:3869-3882.
30. Wu Y, Arai AC, Rumbaugh G, et al. Mutations in ionotropic AMPA receptor 3 alter channel properties and are associated with moderate cognitive impairment in humans. *Proc Natl Acad Sci U S A*. 2007;104:18163-18168.
31. Chérot E, Keren B, Dubourg C, et al. Using medical exome sequencing to identify the causes of neurodevelopmental disorders: Experience of 2 clinical units and 216 patients. *Clin Genet*. 2018;93:567-576.
32. Hamanaka K, Miyoshi K, Sun JH, et al. Amelioration of a neurodevelopmental disorder by carbamazepine in a case having a gain-of-function GRIA3 variant. *Hum Genet*. 2022;141:283-293
33. Rinaldi B, Ge YH, Freri E, et al. Myoclonic status epilepticus and cerebellar hypoplasia associated with a novel variant in the GRIA3 gene. *Neurogenetics*. 2022;23:27-35.
34. Sun JH, Chen J, Ayala Valenzuela FE, et al. X-linked neonatal-onset epileptic encephalopathy associated with a gain-of-function variant p.R660T in GRIA3. *PLoS Genet*. 2021;17:e1009608.
35. Martinez-Esteve Melnikova A, Pijuan J, Aparicio J, et al. The p.Glu787Lys variant in the GRIA3 gene causes developmental and epileptic encephalopathy mimicking structural epilepsy in a female patient. *Eur J Med Genet*. 2022;65:104442.
36. Philippe A, Malan V, Jacquemont ML, et al. Xq25 duplications encompassing GRIA 3 and STAG 2 genes in two families convey recognizable X-linked intellectual disability with distinctive facial appearance. *Am J Med Genet A*. 2013;161:1370-1375.
37. Chiyonobu T, Hayashi S, Kobayashi K, et al. Partial tandem duplication of GRIA3 in a male with mental retardation. *Am J Med Genet A*. 2007;143:1448-1455.
38. Allen NM, Conroy J, Shahwan A, et al. Unexplained early onset epileptic encephalopathy: Exome screening and phenotype expansion. *Epilepsia*. 2016;57:e12-e17.
39. Jacquemont ML, Sanlaville D, Redon R, et al. Array-based comparative genomic hybridisation identifies high frequency of cryptic chromosomal rearrangements in patients with syndromic autism spectrum disorders. *J Med Genet*. 2006;43:843-849.
40. Guilmatre A, Dubourg C, Mosca AL, et al. Recurrent rearrangements in synaptic and neurodevelopmental genes and shared biologic pathways in schizophrenia, autism, and mental retardation. *Arch Gen Psychiatry*. 2009;66:947-956.
41. Bonnet C, Leheup B, Béri M, Philippe C, Grégoire MJ, Jonveaux P. Aberrant GRIA3 transcripts with multi-exon duplications in a family with X-linked mental retardation. *Am J Med Genet A*. 2009;149:1280-1289.
42. Yang Y, Muzny DM, Xia F, et al. Molecular findings among patients referred for clinical whole-exome sequencing. *JAMA*. 2014;312:1870-1879.
43. Hu H, Haas SA, Chelly J, et al. X-exome sequencing of 405 unresolved families identifies seven novel intellectual disability genes. *Mol Psychiatry*. 2016;21:133-148.
44. LaDuca H, Farwell KD, Vuong H, et al. Exome sequencing covers >98% of mutations identified on targeted next generation sequencing panels. *PLoS One*. 2017;12:e0170843.
45. Hesse AN, Bevilacqua J, Shankar K, Reddi HV. Retrospective genotype-phenotype analysis in a 305 patient cohort referred for testing of a targeted epilepsy panel. *Epilepsy Res*. 2018;144:53-61.
46. Lyu Y, Yang Y, Liu Y, Gai Z. Analysis of a patient with X-linked mental retardation by next generation sequencing. *Zhonghua Yi Xue Yi Chuan Xue Za Zhi*. 2018;35:257-260.
47. Bai Z, Kong X. X-linked mental retardation combined with autism caused by a novel hemizygous mutation of GRIA3 gene. *Zhonghua Yi Xue Yi Chuan Xue Za Zhi*. 2019;36:829-833.

48. Carraro M, Monzon AM, Chiricosta L, et al. Assessment of patient clinical descriptions and pathogenic variants from gene panel sequences in the CAGI-5 intellectual disability challenge. *Hum Mutat*. 2019;40:1330-1345.
49. Fernández-Marmiesse A, Roca I, Díaz-Flores F, et al. Rare variants in 48 genes account for 42% of cases of epilepsy with or without neurodevelopmental delay in 246 pediatric patients. *Front Neurosci*. 2019;13:1135.
50. Poot M, Eleveld MJ, van 't Slot R, Ploos van Amstel HK, Hochstenbach R. Recurrent copy number changes in mentally retarded children harbour genes involved in cellular localization and the glutamate receptor complex. *Eur J Hum Genet*. 2010;18:39-46.
51. Alkelai A, Shohat S, Greenbaum L, et al. Expansion of the GRIA2 phenotypic representation: A novel de novo loss of function mutation in a case with childhood onset schizophrenia. *J Hum Genet*. 2021;66:339-343.
52. Latsko MS, Koboldt DC, Franklin SJ, et al. De novo missense mutation in GRIA2 in a patient with global developmental delay, autism spectrum disorder, and epileptic encephalopathy. *Cold Spring Harb Mol Case Stud*. 2022;8:a006172.
53. Vijayaraghavan A, Urulangodi M, Ajit Valaparambil K, Sundaram S, Krishnan S. Movement disorders in GRIA2-related disorder – expanding the genetic spectrum of developmental dyskinetic encephalopathy. *Mov Disord Clin Pract*. 2023;10:1222-1224.
54. Cai Q, Zhou Z, Luo R, et al. Novel GRIA2 variant in a patient with atypical autism spectrum disorder and psychiatric symptoms: A case report. *BMC Pediatr*. 2022;22:629.
55. Okano S, Makita Y, Miyamoto A, et al. GRIA3 p.Met661Thr variant in a female with developmental epileptic encephalopathy. *Hum Genome Var*. 2023;10:1-4.
56. Wang H, Liu J, Li F, Teng Z, Liu M, Gu W. Novel heterozygous missense variant in GRIA4 gene associated with neurodevelopmental disorder with or without seizures and gait abnormalities. *Front Genet*. 2022;13:859140.
57. Ismail V, Zachariassen LG, Godwin A, et al. Identification and functional evaluation of GRIA1 missense and truncation variants in individuals with ID: An emerging neurodevelopmental syndrome. *Am J Hum Genet*. 2022;109:1217-1241.
58. Firth HV, Richards SM, Bevan AP, et al. DECIPHER: Database of chromosomal imbalance and phenotype in humans using Ensembl resources. *Am J Hum Genet*. 2009;84:524-533.
59. Landrum MJ, Lee JM, Benson M, et al. ClinVar: Improving access to variant interpretations and supporting evidence. *Nucleic Acids Res*. 2018;46:D1062-D1067.
60. Sobreira N, Schiettecatte F, Valle D, Hamosh A. GeneMatcher: A matching tool for connecting investigators with an interest in the same gene. *Hum Mutat*. 2015;36:928-930.
61. Peng SX, Pei J, Rinaldi B, et al. Dysfunction of AMPA receptor GluA3 is associated with aggressive behavior in human. *Mol Psychiatry*. 2022;27:4092-4102.
62. Kiskin NI, Krishtal OA, Tsyndrenko AY. Excitatory amino acid receptors in hippocampal neurons: Kainate fails to desensitize them. *Neurosci Lett*. 1986;63:225-230.
63. Otis T, Zhang S, Trussell LO. Direct measurement of AMPA receptor desensitization induced by glutamatergic synaptic transmission. *J Neurosci*. 1996;16:7496-7504.
64. Stern-Bach Y, Russo S, Neuman M, Rosenmund C. A point mutation in the glutamate binding site blocks desensitization of AMPA receptors. *Neuron*. 1998;21:907-918.
65. Suzuki E, Kessler M, Arai AC. The fast kinetics of AMPA GluR3 receptors is selectively modulated by the TARPs gamma 4 and gamma 8. *Mol Cell Neurosci*. 2008;38:117-123.
66. Pei W, Huang Z, Niu L. Glur3 flip and flop: Differences in channel opening kinetics. *Biochemistry*. 2007;46:2027-2036.
67. Silk M, Petrovski S, Ascher DB. MTR-Viewer: Identifying regions within genes under purifying selection. *Nucleic Acids Res*. 2019;47:W121-W126.
68. Magazanik LG, Buldakova SL, Samoilova MV, Gmiro VE, Mellor IR, Usherwood PNR. Block of open channels of recombinant AMPA receptors and native AMPA/kainate receptors by adamantane derivatives. *J Physiol*. 1997;505:655-663.
69. Hampson DR, Manalo JL. The activation of glutamate receptors by kainic acid and domoic acid. *Nat Toxins*. 1998;6:153-158.
70. Tsubokawa H, Oguro K, Masuzawa T, Nakaima T, Kawai N. Effects of a spider toxin and its analogue on glutamate-activated currents in the hippocampal CA1 neuron after ischemia. *J Neurophysiol*. 1995;74:218-225.
71. Koike M, Iino M, Ozawa S. Blocking effect of 1-naphthyl acetyl spermine on Ca(2+)-permeable AMPA receptors in cultured rat hippocampal neurons. *Neurosci Res*. 1997;29:27-36.
72. Twomey EC, Yelshanskaya MV, Vassilevski AA, Sobolevsky AI. Mechanisms of channel block in calcium-permeable AMPA receptors. *Neuron*. 2018;99:956-968.e4.
73. Traynelis J, Silk M, Wang Q, et al. Optimizing genomic medicine in epilepsy through a gene-customized approach to missense variant interpretation. *Genome Res*. 2017;27:1715-1729.
74. Zhao Y, Chen S, Swensen AC, Qian WJ, Gouaux E. Architecture and subunit arrangement of native AMPA receptors elucidated by cryo-EM. *Science*. 2019;364:355-362.
75. Schwenk J, Harmel N, Brechet A, et al. High-resolution proteomics unravel architecture and molecular diversity of native AMPA receptor complexes. *Neuron*. 2012;74:621-633.
76. van der Spek SJF, Pandya NJ, Koopmans F, et al. Expression and interaction proteomics of GluA1- and GluA3-subunit-containing AMPARs reveal distinct protein composition. *Cells*. 2022;11:3648.
77. Wenthold RJ, Petralia RS, Blahos J, Niedzielski AS. Evidence for multiple AMPA receptor complexes in hippocampal CA1/CA2 neurons. *J Neurosci*. 1996;16:1982-1989.
78. Sommer B, Keinänen K, Verdoorn TA, et al. Flip and flop: A cell-specific functional switch in glutamate-operated channels of the CNS. *Science*. 1990;249:1580-1585.
79. Monyer H, Seeburg PH, Wisden W. Glutamate-operated channels: Developmentally early and mature forms arise by alternative splicing. *Neuron*. 1991;6:799-810.
80. Strehlow V, Heyne HO, Vlaskamp DRM, et al. GRIN2A-related disorders: Genotype and functional consequence predict phenotype. *Brain*. 2019;142:80-92.
81. Wolff M, Johannesen KM, Hedrich UBS, et al. Genetic and phenotypic heterogeneity suggest therapeutic implications in SCN2A-related disorders. *Brain*. 2017;140:1316-1336.
82. Brunklaus A, Du J, Steckler F, et al. Biological concepts in human sodium channel epilepsies and their relevance in clinical practice. *Epilepsia*. 2020;61:387-399.
83. Brunklaus A, Schorge S, Smith AD, et al. SCN1A variants from bench to bedside-improved clinical prediction from functional characterization. *Hum Mutat*. 2020;41:363-374.
84. Masnada S, Hedrich UBS, Gardella E, et al. Clinical spectrum and genotype-phenotype associations of KCNA2-related encephalopathies. *Brain*. 2017;140:2337-2354.
85. Johannesen KM, Liu Y, Koko M, et al. Genotype-phenotype correlations in SCN8A-related disorders reveal prognostic and therapeutic implications. *Brain*. 2022;145:2991-3009.
86. Malerba F, Alberini G, Balagura G, et al. Genotype-phenotype correlations in patients with de novo KCNQ2 pathogenic variants. *Neurol Genet*. 2020;6:e528.

87. Benke TA, Park K, Krey I, et al. Clinical and therapeutic significance of genetic variation in the GRIN gene family encoding NMDARs. *Neuropharmacology*. 2021;199:108805.
88. Han W, Yuan H, Allen JP, et al. Opportunities for precision treatment of GRIN2A and GRIN2B gain-of-function variants in triheteromeric N-methyl-D-aspartate receptors. *J Pharmacol Exp Ther*. 2022;381:54-66.
89. Absalom NL, Liao VWY, Johannesen KMH, et al. Gain-of-function and loss-of-function GABRB3 variants lead to distinct clinical phenotypes in patients with developmental and epileptic encephalopathies. *Nat Commun*. 2022;13:1822.
90. Migeon BR. X-linked diseases: Susceptible females. *Genet Med*. 2020;22:1156-1174.
91. Srivastava S, Love-Nichols JA, Dies KA, et al. Meta-analysis and multidisciplinary consensus statement: Exome sequencing is a first-tier clinical diagnostic test for individuals with neurodevelopmental disorders. *Genet Med*. 2019;21:2413-2421.
92. Krey I, Platzer K, Esterhuizen A, et al. Current practice in diagnostic genetic testing of the epilepsies. *Epileptic Disord*. 2022;24:765-786.
93. Brünger T, Pérez-Palma E, Montanucci L, et al. Conserved patterns across ion channels correlate with variant pathogenicity and clinical phenotypes. *Brain*. 2023;146:923-934.
94. Arai AC, Kessler M. Pharmacology of ampakine modulators: From AMPA receptors to synapses and behavior. *Curr Drug Targets*. 2007;8:583-602.
95. Goff DC, Lamberti JS, Leon AC, et al. A placebo-controlled add-on trial of the Ampakine, CX516, for cognitive deficits in schizophrenia. *Neuropsychopharmacology*. 2008;33:465-472.
96. Wesensten NJ, Reichardt RM, Balkin TJ. Ampakine (CX717) effects on performance and alertness during simulated night shift work. *Aviat Space Environ Med*. 2007;78:937-943.
97. Senin U, Abate G, Fieschi C, et al. Aniracetam (Ro 13-5057) in the treatment of senile dementia of Alzheimer type (SDAT): Results of a placebo controlled multicentre clinical study. *Eur Neuropsychopharmacol*. 1991;1:511-517.
98. Olson ME, Eubanks LM, Janda KD. Chemical interventions for the opioid crisis: Key advances and remaining challenges. *J Am Chem Soc*. 2019;141:1798-1806.
99. Lynch G, Gall CM. Ampakines and the threefold path to cognitive enhancement. *Trends Neurosci*. 2006;29:554-562.
100. Yuan CL, Shi EY, Srinivasan J, Ptak CP, Oswald RE, Nowak LM. Modulation of AMPA receptor gating by the anticonvulsant drug, perampanel. *ACS Med Chem Lett*. 2019;10:237-242.
101. Potschka H, Trinka E. Perampanel: Does it have broad-spectrum potential? *Epilepsia*. 2019;60(Suppl 1):22-36.
102. Coombs ID, Ziobro J, Krotov V, Surtees TL, Cull-Candy SG, Farrant M. A gain-of-function GRIA2 variant associated with neurodevelopmental delay and seizures: Functional characterization and targeted treatment. *Epilepsia*. 2022;63:e156-e163.
103. Jackson AC, Nicoll RA. The expanding social network of ionotropic glutamate receptors: TARPs and other transmembrane auxiliary subunits. *Neuron*. 2011;70:178-199.
104. Schwenk J, Fakler B. Building of AMPA-type glutamate receptors in the endoplasmic reticulum and its implication for excitatory neurotransmission. *J Physiol*. 2021;599:2639-2653.